# Armed Services Technical Information Agency

## ARLINGTON HALL STATION
## ARLINGTON 12 VIRGINIA

FOR

MICRO-CARD

CONTROL ONLY

[1] OF [2]

State University of New York College of Ceramics

at

Alfred University, Alfred, New York

## PHOTOCONDUCTIVITY
## IN CADMIUM TELLURIDE

July 1958

Contract Nonr 1503(01)

Project No. NR 015-215

T. J. Gray

Project Director

THE PREPARATION AND MEASUREMENT OF THE PHOTOCONDUCTIVITY OF

CADMIUM TELLURIDE SINGLE CRYSTALS


by

Clyde Emerson McNeilly, B.S.


A Dissertation

submitted in candidacy

for the degree of

Doctor of Philosophy

in

Ceramics

at

Alfred University


State University of New York

College of Ceramics


July 1958

THE PREPARATION AND MEASUREMENT OF THE PHOTOCONDUCTIVITY OF

CADMIUM TELLURIDE SINGLE CRYSTALS

ABSTRACT

Single crystals of cadmium telluride with an impurity concentra-
tion of about $10^{17}$ cc$^{-3}$ have been prepared from zone purified tellurium
and high purity cadmium by a modified Stockbarger process. Apparatus and
techniques for zone refining and crystal growth are described.

Crystals were prepared for measurement by cutting on either an
S. S. White Industrial Airbrasive unit or carborundum disks followed by
removal of the surface layer with the "airbrasive". Vacuum plated indium
electrodes were used on n-type crystals while gold deposited from gold
chloride solution was used on p-type.

Although thermal emf measurements show pure CdTe to be p-type,
it was found necessary to use indium contacts as the gold chloride greatly
altered the photoconductivity of the specimens. Thermal activation energy
measurements indicate an intrinsic activation energy of 1.5 eV in the
temperature range $350^{\circ}$ – $20^{\circ}$C.

A Perkin Elmer Model 83 single-beam double-pass monochromator
equipped with rock salt optics and a Glo-bar operated at $1600^{\circ}$K was used
as the radiation source in the wavelength region 0.6 to 12 microns.

The wavelength for maximum intrinsic photoconductivity is given
by the expression:

$$\lambda(\text{Å}) = 8100 + 2.06\ T$$

which in turn gives an intrinsic activation energy of:

$$\Delta e\ (eV) = 1.53 - 0.00035T$$

Photoconductivity measurements indicate another activation energy of about 1.1 eV for pure CdTe. This has been shown to arise from a level 0.4 eV above the valence band and correlates with the levels found at 1.0 eV and 0.64 eV above the valence band in pure CdS and CdSe, respectively.

Dependence of maximum photocurrent and variation of rise time with radiation intensity and temperature show a slightly supralinear character and indicate the presence of discrete levels scattered between the top of the valence band and the 0.4 eV level.

The model proposed for CdTe including two types of levels explains quite well the photoconducting properties as related to temperature dependence, supralinearity, and speed of response as encountered in this material, and follows closely the semiquantitative evaluation of photoconductivity in CdS and CdSe given by Rose.

## ACKNOWLEDGMENT

## TABLE OF CONTENTS

# 1.0 INTRODUCTION

Among the more basic properties of semiconductors and
insulators, photoconductivity is perhaps one of the most useful
in determining a detailed account of the energy level model of a
solid. The variation of photocurrent and its rise time with tem-
perature, intensity of radiation, wavelength, and even illumination
history can lead to an interpretation of the distribution of traps,
recombination centers and other types of discrete levels, both
normally filled and unfilled, in the forbidden zone, along with a
description of their other properties.

From this variety of information which may be obtained
from photoconductivity measurements one can readily appreciate
that photoconductivity is an extremely complex phenomena; the
photocurrent possibly increasing in a linear, supralinear, or sub-
linear fashion with increasing radiation intensity. It may likewise
increase, decrease, or possibly stay constant with increasing tem-
perature. Along with these effects must be included those due to
voltage dependence, impurities, both intentional and unavoidable,
surface effects, and history of treatment before and during
measurement. From these considerations it is apparent that great
difficulty will be encountered in deriving and applying a general
all-inclusive theory of photoconductivity. As a result, the
general trend has been to investigate a group of common materials
such as the alkali halides, or crystals with the zincblende struc-
ture and to assemble the data into a theory consistent for that
particular type photoconductor.

Although photoconductivity in zinc sulfide natural crystals
and artifically prepared powders, both pure and impure, had been inves-
tigated as early as 1920 by Gulden and Pohl (1), the most extensive
interpretive investigations of photoconductivity were made on alkali
halide crystals in the 1930's. These materials were readily available
in single crystal form and a variety of defects could be added at will,
by high energy radiation and heating in a vapor of the cation or anion.

However, with the advent of increasing interest in semicon-
ductors since the 1940's brought about by the development of transistors,
radiation detectors, and other semiconductor devices, a wealth of
information concerning the phenomena of photoconductivity has become
available. No entirely satisfactory overall description of photo-
conductivity yet exists, however, from which the behavior of any given
semiconductor under illumination may be predicted.

From the previously mentioned aspects of photoconductivity
one can anticipate that the exact nature of the material being inves-
tigated must be clearly defined and free from disturbing influences.
To attain this end it is necessary to have (1) as low as possible a
level of impurity ions, (2) as near as possible perfect crystal
structure, and (3) ideal stoichiometry.

Among the first semiconducting compounds to be examined
were the group II-VI combinations, consisting of the sulfides, selen-
ides, and tellurides of zinc, cadmium, and mercury.

High purity cadmium and zinc (99.9997%) were readily
available and since considerable work was being carried out on
the sulfides and only slightly less on the selenides, the tellurides
were chosen for this investigation. Cadmium telluride in particular

seemed to lend itself readily to the Stockbarger crystal growth pro ess
and it was anticipated that photoconductivity data from CdTe single
crystals might be correlated to that available from CdS ꞏ ꞏꞏ ꞏdSe. Also,
it was established that the technique of zone refining could be applied
to tellurium, resulting in tellurium in a state of purity at least com-
parable to that of the cadmium and zinc.

A more detailed treatment of the theory of zone refining and
its applications to tellurium, selenium, and sulfur will be given later.
The aspects of crystal growth as have been encountered in these materials
will also be reviewed with particular emphasis on the methods developed
here for CdTe and ZnTe.

These considerations will be followed by a general account of
photoconductivity and, more particularly, a detailed discussion of the
band model for CdTe and its interpretation as derived from photoconduc-
tivity measurements, and its relation to photoconductivity as observed
in CdS and CdSe.

2.0   ZONE REFINING

## 2.1 Introduction

Although a perfect single crystal, from the point of view of
both structure and composition is theoretically non-existent, the closer
one can approach it, the more reliable will be the observations made
upon it. Of the major defects normally found in crystals, perhaps the
most troublesome and the one over which the greatest control can be
exercised is the presence of foreign atoms or ions in substitutional
or interstitial sites. Nowhere is this of greater importance than in
the field of semiconductors where the presence of impurities in concen-
trations on the order of parts per million or less may completely alter
the electrical conductivity process in the crystal. The quest for a
more perfect crystal free from this type of defect has lead to the devel-
opment of certain specialized techniques, one of the most useful of
which is zone refining (2).

Zone refining is based on the principle of impurity segre-
gation which has long been the basis of purification by repeated
fractional crystallization. In fractional crystallization, however,
the entire batch is melted, whereas with zone melting only a small
segment of the batch is molten at any one time.

The phenomena of impurity segregation results from the
difference in solute concentration between the freezing solid and
the liquid in contact with it, which in turn arises from the equilib-
rium between the solid and liquid in a binary solid solution system.
While in practice, the molten zone will most likely not be in equilib-
rium with the entire solid, if the rate of zone movement; that is, the

rate of movement of the interface, is properly chosen, near equilibrium conditions will prevail at the interface, and separation of the solute will occur. This rate has been empirically determined to be from one to 25 cm/hr, for most metals and semiconductors.

If we now examine the very end region of the two possible types of phase diagrams for the binary systems composed of the material in which we are interested and the impurity or solute material, we can graphically demonstrate the difference in solute concentration between the liquid and solid.



(a)                                    (b)
Impurity Concentration
Figure 1
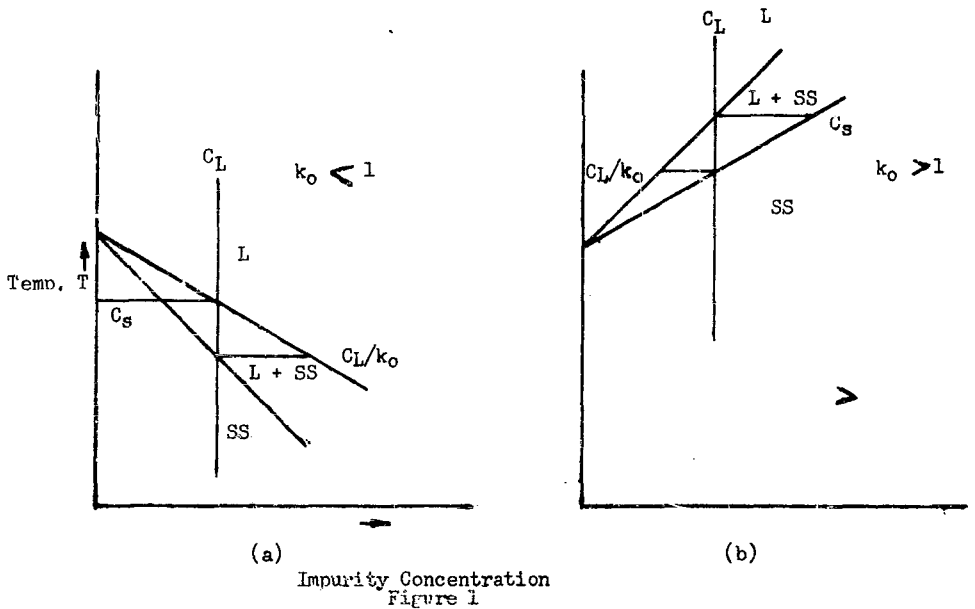
The liquidus and solidus are probably not straight lines as shown, but since we are interested in only such a small region no appreciable error is introduced in drawing them as such. In figure 1a, the

solute is more soluble in the liquid than the solid, and so the ratio of $C_S/C_L$ is less than unity, where $C_S$ and $C_L$ are the concentration of solute in the solid and liquid, respectively. This ratio is designated as the equilibrium distribution coefficient, $k_o$.

Consider now the equilibrium crystallization of a composition on the line $C_L$, in figure 1a (figure 1b will be analagous except the solute is more soluble in the solid). At temperature T the first solid to crystallize out will have a solute concentration of $C_S$, ($C_L k_o$). As cooling continues the composition of the solid, assuming complete equilibrium, will shift along the solidus till it reaches the line $C_L$ at which time it will be completely solid. Since the diffusion solids is low, this equilibrium will generally not be attai as is usually the case, the rate of travel of the interface is large compared to the rate of diffusion, the impurity will concentrate in the liquid. This, of course, assumes the rate of diffusion in the liquid is sufficiently larger than the rate of interface travel, or that mixing is present to keep an impurity enriched layer from building up in the liquid at the interface. In the usual zone melting methods thermal gradients will certainly be present which will significantly aid in mixing the liquid. For efficient zone refining, however, the rate of travel may well be fast enough that such a lyer does in fact form. When this occurs it is no longer the equilibrium distribution coefficient which determines the purification process, but the effective distribution coefficient. This is given by Burton et al (3).

$$k = \frac{k_o}{k_o + (1 - k_o)\, e^{\frac{-fd}{D}}} \tag{1}$$

$k$ = effective distribution coefficient,

$f$ = growth rate,

$d$ = liquid film thickness in which solute transport is by diffusion only,

$D$ = diffusivity in liquid.

The quantity $fd/D$ is designated as a growth parameter and as it increases, $k$ will approach unity regardless of the value of $k_0$. For efficient zone melting then, since $D$ and, to some extent, $d$ are fixed properties of the liquid a small growth rate is desirable. While $k_0$ and hence $k$, should theoretically be available from phase diagrams, most presently available diagrams are not of sufficient accuracy for this. Thurmond and Struthers (4) have developed a relation between $k_0$ and temperature from solution concentration relations. A thermodynamic approach based on dilute solutions has been made by Hayes and Chipman (5).

In the final analysis, however, where one wishes to rid one element of many impurities the most reliable procedure is to actually zone melt the material and run standard analysis after different numbers of zones have been passed through it at different rates.

Let us now consider the effect on the impurity level of actually passing a molten zone through a rod of material. We will pass a zone of length L along a bar, of cross section A, with an initial impurity concentration $C_0$ and effective distribution coefficient $k < 1$. As the molten zone moves forward, solid with an impurity concentration of $kC_0$ will freeze out behind. In a distance $dx$ then, an amount of impurity equal to $kC_0Adx$ will have frozen out in the solid while an amount $C_cAdx$ will have been dissolved into the

liquid. Thus the initial solid is decreased in impurity content while the liquid is increased. As the molten zone continues to move, the impurity concentration of both the liquid and solid will increase until the concentration in the liquid has reached $C_0/k$ at which time the solid freezing out will have the same composition as that melting. No change in solute concentration will occur as the zone continues moving until it reaches the end of the bar where all the solute will be deposited. The impurity distribution will then be as represented in figure 2.
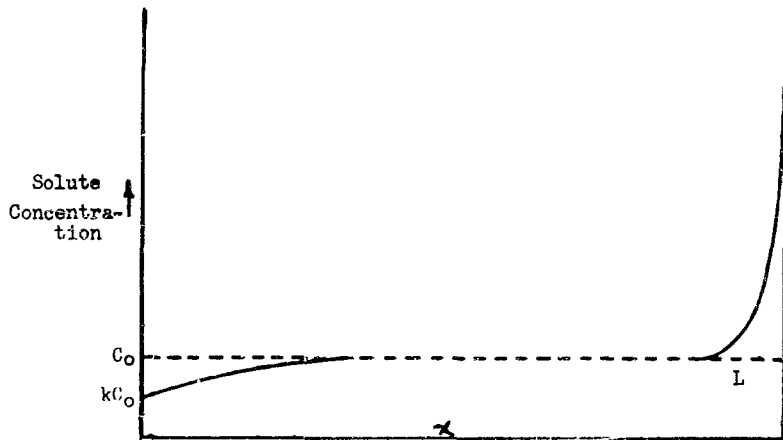


Figure 2

The net area between the $C_0$ line and the curve after the pass must of course be zero. Because of this the solute concentration in the final length L of the bar will rise quite sharply as the initial length of partially purified material may extend for a distance much greater than L. Read (6) has derived an equation representing the impurity distribution valid up to a distance L from the end as shown in figure 2.

$$\frac{C}{C_0} = 1 - (1 - k) e^{-kx/L} \qquad (2)$$

C = solute concentration in solid,

x = distance from front end of bar.

If a second pass is now made through the rod, the initial solid would have a concentration of $k^2C_0$, since the starting concentration was $kC_0$. The length of the partially purified section will also increase as will the final impure region. As more and more passes are made, the region of constant solute concentration, $C_0$, will disappear and the distribution curves will take on the forms shown in figure 3.
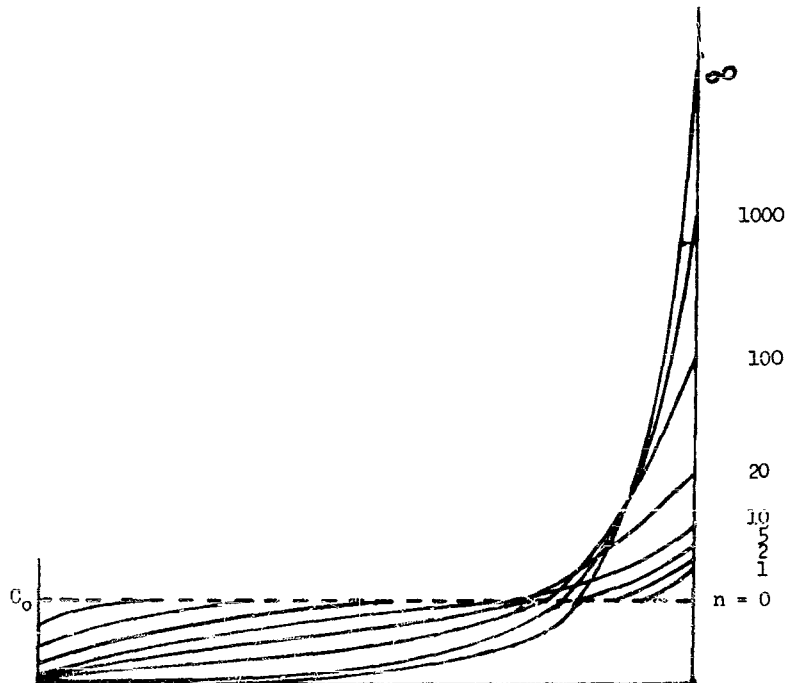


Figure 3

These curves are of course merely typical representations, the actual shape after any given number of passes depending on k and the ratio of zone length to overall length.

While it might be anticipated that the starting end of the rod would approach a zero level of impurities, this possibility is prohibited by contamination and diffusion; contamination coming from the boat and the atmosphere surrounding it. A steady state is thus reached at which the impurities are entering the material as fast as they are being swept out.

The above discussion was concerned with systems for which k is less than unity. Similar arguments apply for k greater than unity. In this case, however, the impurity concentration build-up occurs in the starting region.

For more efficient application of zone refining a series of closely spaced heaters is used to effect the purification rather than one heater. Thus, for example, a series of four heaters on four-inch centers traveling two inches an hour can effectively pass one complete zone through a sixteen-inch specimen every two hours rather than the eight hours required by the one heater.

## 2.2 General Applications

From the foregoing discussion certain factors may be selected for consideration in attempting to zone refine any given material. Since the value of k is the controlling factor in determining the purification, the values for growth rate (f) and diffusion film thickness (d) upon which k depends must be selected with care. Zone spacing and length must also be considered. Efficiency considerations

would call for a short pass time, which might be achieved by increasing f, or decreasing zone length and separation. If f is increased, however, k will approach unit and purification efficiency will fall off. Decreasing d by stirring, however, may permit an increase in f without affecting k. Once the value for f is chosen, the number of passes needed to attain a certain purity level will be fixed, and so the value for zone length and spacing can be adjusted to give optimum pass time and cost of operation. The selection of the actual physical requirements for zone refining must likewise be given careful consideration. Two general procedures are available; each presenting its own particular problems.

(1) Zone purifying in a container:

In this case the choice of a container material which will not contaminate the melt is obviously of greatest importance. Contamination may arise from direct reaction or solution between the container and the melt, impurities included in the boat material, or adsorbed gases on the surface of the boat. A low thermal conductivity in the boat is also necessary for good control of the zone length. There should not be too great a difference between the thermal expansions of the container and the material being refined. A carefully chosen and controlled atmosphere must be maintained over the melt to prevent contamination. A thoroughly purified noble gas will usually be sufficient.

The heat necessary to maintain the molten zones may be supplied by numerous means; resistance, induction, focused infrared or sunlight, or even gas flames, are a few. For elements such as gallium (7) or mercury, refrigerated coils can be employed to separate the molten zones. In the usual laboratory batch operation a series

of reciprocating resistance or induction heaters is usually adequate.

(2) Zone purifying without a container:

In cases where a material has too high a melting point or is too reactive to be contained in a boat, several specialized techniques have been developed. One of the most obvious is to use the material itself as its own container. This may be accomplished by forced cooling of the sides and bottom of the specimen or shallow heating. The unpurified material may then be mechanically removed or purified in a subsequent operation. Other processes rely mainly on passing through the solid rod a molten zone held in place by its surface tension. This method was apparently developed independently by several workers, but was first described by Keck and Golay (8), who applied it to silicon. Induction heating is generally used to produce the molten zone although various types of resistance heaters have been used.

Other variations in this technique include use of a magnetic field to support the molten zone in a horizontal rod (9) and use of square rods in which the corners do not melt with induction heating and so form a support for the molten zone (10).

2.3 Application to Tellurium, Selenium and Sulfur

For the growth of high purity CdTe and ZnTe single crystals suitable for photoconductivity measurements, a high state of purity in the raw materials was necessary, since the finished CdTe or ZnTe cannot be purified itself owing to a great tendency to dissociate upon melting. It was therefore necessary to zone refine the tellurium and since meager data was available for selenium and sulfur, they were also included. From their reasonably low melting points (Te - 452°, Se - 200°

$S - 115^\circ C$), it was decided that a reciprocating series of resistance heaters acting on a straight rod of material would be adequate. The phase diagrams for these elements and the variety of impurities usually associated with them were not generally available so the values for zone length, spacing and rate of travel were arbitrarily selected to be one-inch heaters spaced four inches apart with an interface rate of travel of two inches per hour. With this arrangement, using a specimen of about one-half square inch cross section and s... ...ches long, about 100 grams "pure" material was obtained after ... passes.

First attempts at refining used a moving sealed "Vycor" tube about 90 percent full, and stationary heaters. Almost invariably these tubes broke after several passes as did silica tubes which were also tried. As a result of this the entire unit was redesigned to use moving heaters (figure 4). In this apparatus the boat could be placed inside a fixed silica tube with a protective atmosphere or evacuated, so the material would not be contaminated in the event the container did break. Because of the high vapor pressure of these elements at their melting points it was not feasible to refine them under vacuum. An atmosphere of high purity helium introduced into the silica tube after passing through a charcoal trap at liquid nitrogen temperature resulted in a film free surface and apparently introduced no new impurities.

Since "Vycor" and silica were unsatisfactory for a container material, a recrystallized alumina thermocouple protection tube was split longitudinally for use as a boat. This proved entirely satisfactory from a purity standpoint although some inconvenience was

encountered in removing the material as a result of its wetting action. Removal was best accomplished by inverting the filled boat in the outer silica container and running one pass through it. The rod then melted onto the silica from which it was easily removed.

After removal from the boat samples were taken from each four-inch section of the rod for spectrographic analysis to be compared with the starting material. Although high purity materials were originally used for zone refining it was subsequently found, particularly with tellurium, that commercial C.P. grade material could just as readily be reduced to the same final impurity level. A typical zone refined Te specimen before removal from its boat is shown in figure 5.

Some work has been done on the zone refining of other metals to determine the overall adaptability of this particular arrangement. Cadmium, zinc and aluminum were run through this purifier and the greatest difficulty encountered seemed to be due to the relatively high thermal conductivity of these elements. Either the two end zones tended to freeze solid when an inch or more material was outside the end heaters or the interior solid zones melted when enough heat was supplied to keep the end zones molten. Some short-time purifications were made on zinc and aluminum by manually controlling the power to the heaters to maintain the proper zones, but the problem could certainly be eliminated by narrower heaters more widely spaced. Molten aluminum has a sufficiently low vapor pressure to enable it to be zone refined under vacuum, without appreciable volatilization or oxide formation.

Zinc must be placed in the boat in the form of a one-piece rod since the usual granular or chipped zinc has such a heavy film on
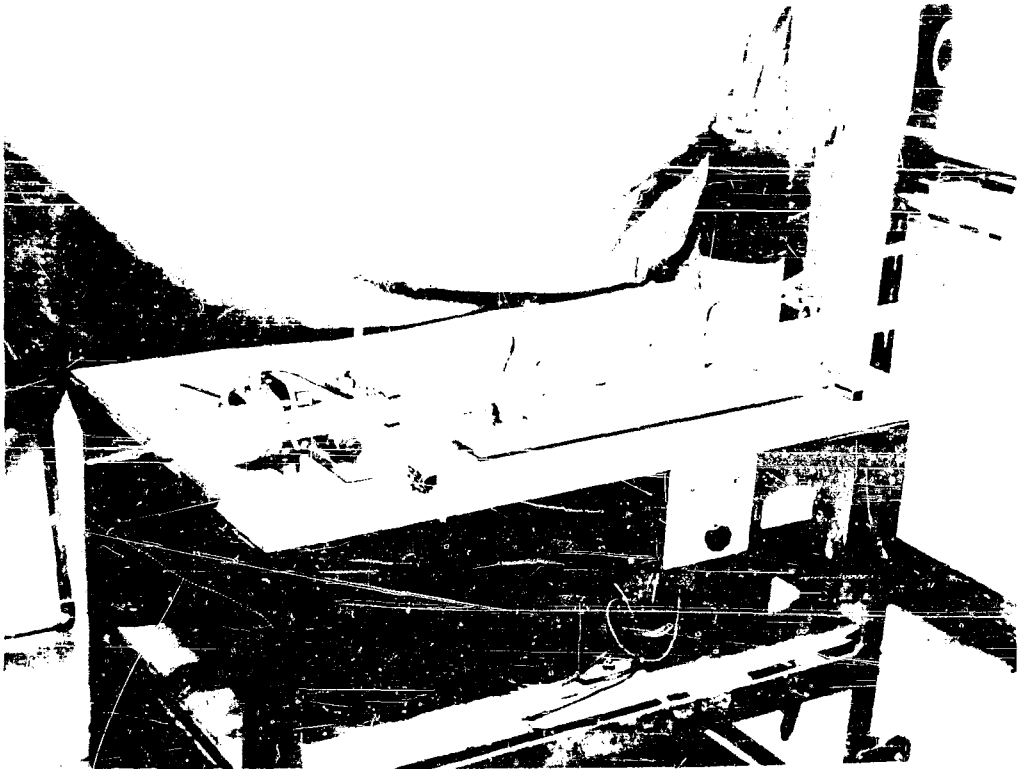
FIGURE 4
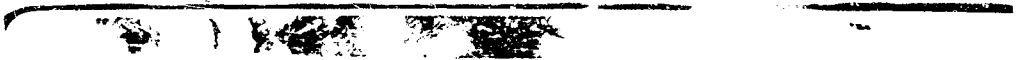
its surface it will not melt together. This problem was also encountered in trying to use tellurium powder as the starting material.

A set of typical spectrographical analyses is given in table I. This data indicates that the principle of zone refining is readily adaptable to the preparation of very pure elements for use in growing single crystals of CdTe and ZnTe.

Table I

| | 1 | 2 | 3 | 4 | 5 | 6 | | 1 | 2 | 3 | 4 | 5 | 6 |
|---|---|---|---|---|---|---|---|---|---|---|---|---|---|
| Ag | Ftr | VVFtr | | | | | Na | VVFtr | BS | | | | |
| Al | | | Ftr | VFtr | tr | BS | Nb | | | | | | |
| As | | | | | BS | BS | Nd | | | | | | |
| Au | | | | | | | Ni | VVFtr | | | | | |
| B | | | | | | | Os | | | | | | |
| Ba | | | | | | | P | | | | | | |
| Be | | | | | | | Pb | VFtr | BS | | | | |
| Bi | | | | | | | Pd | | | | | | |
| Ca | VFtr | VVFtr | | | | | Pr | | | | | | |
| Co | | | | | | | Pt | | | | | | |
| Cd | | | | | | | Ra | | | | | | |
| Ce | | | | | | | Rh | | | | | | |
| Co | | | | | | | Ru | | | | | | |
| Cr | | | | | | | S | | | | | | |
| Cs | | | | | | | Sb | | | | | | |
| Cu | Ftr | | Ftr | Ftr | BS | BS | Sc | | | | | | |
| Dy | | | | | | | Se | | | M | M | | |
| Er | | | | | | | Si | Ftr | VFtr | tr | BS | tr | BS |
| Eu | | | | | | | Sm | | | | | | |
| F | | | | | | | Sn | | | | | | |
| Fe | Ftr | VFtr | VFtr | BS | BS | BS | Sr | | | | | | |
| Ga | | | | | | | Ta | | | | | | |
| Gd | | | | | | | Tb | | | | | | |
| Ge | | | | | | | Te | M | M | | | | |
| Hf | | | | | | | Th | | | | | | |
| Hg | VFtr | | | | | | Ti | | | BS | BS | BS | BS |
| Ho | | | | | | | Tl | | | | | | |
| In | | | | | | | Tm | | | | | | |
| Ir | | | | | | | U | | | | | | |
| K | | | | | | | V | | | | | | |
| La | | | | | | | W | | | | | | |
| Li | | | | | | | Yb | | | | | | |
| Lu | | | | | | | Y | | | | | | |
| Mg | VFtr | VVFtr | | | Ftr | BS | Zn | VVFtr | | | | | |
| Mn | BS | BS | Ftr | BS | | | Zr | | | | | | |
| Mo | | | | | | | | | | | | | |

1. original tellurium (C.P.)
2. purified tellurium (60 passes)
3. original selenium (high purity)
4. purified selenium (35 passes)
5. original sulfur (C.P.)
6. purified sulfur (35 passes)

M     - Major constituent
tr    - trace
Ftr   - faint trace
VFtr  - very faint trace
VVFtr - very very faint trace
BS    - barely shows

## 3.0 CRYSTAL GROWTH

### 3.1 Introduction

When a sufficient quantity of high purity material is available
the problem of transforming it into single crystals must then be con-
sidered. The four general processes available for crystal growth are
the phase transformations vapor-solid, liquid-solid, and solid-solid,
and crystallization from solution. For semiconductors, the most readily
applicable from a consideration of their physical properties and the
most commonly used, are the vapor phase and  uid phase transformations.

A brief consideration of the aspects of actual crystal formation
is first desirable regardless of the method of formation. J. W. Gibbs
presented a qualitative theory of crystal growth based on thermodynam-
ical reasoning in the latter 1800's, but the theory put forth by
Curie (11) in 1885 was the first to gain prominent recognition by
crystallographers (12). This theory preceeded the atomic picture as
we now know it and was instead based on the relationship between
crystalline form and surface energy of a solid, the proper crystal-
line form being that which gave the lowest energy. Several workers
including Hilton (13) and Wulff (14) extended this theory but shortly
after, Berthoud (15) showed that this approach predicted the more
rapid a crystal grew the more complex its form would become, when in
fact the opposite is true. Since then many theories have been devel-
oped, the more recent ones having been evolved from a consideration
of defect structure. Buckley (12) presents a historical compilation
of the many possibilities presented throughout th  1920's and 30's,
based for the most part on the writings of Smekal and Zwicky. The
present status of theory is a synthesis of generally accepted ideals

based on theoretical considerations and empirical facts.

Generally, and it might be added ideally, crystals may be pictured as an orderly arrangement of atoms (as spheres) in a repetitious three-dimensional structure, with a fundamental unit used as the pattern of repetition. Throughout this arrangement, in different directions there must then be different sets of planes of atoms. In crystal growth once a lattice face is formed, atoms will be arriving at and leaving from this plane at equal rates, assuming equilibrium conditions. Once an atom strikes the surface next to an already bound atom, however, it will have a greater tendency to remain there since it is now "bound" in two places and will thus have lower energy. As this process is repeated a "step" will be built up and continue to propagate over the surface until a new plane is completed. "Nucleation" of a plane may occur in several splaces and if anything arises such as a previous dislocation or a foreign atom entering the structure, a dislocation will occur where the nuclei grow together. The presence of such dislocations as a prerequisite for continuing crystal growth has been called for in the theory of Frank (16).

Although these observations apply to crystals in general, further considerations will depend on the nature of crystal growth and the particular habits of the individual crystal.

## 3.2 Growth from Melt

The wide variety of crystals with an even wider variety of properties which may be grown from the melt has lead to almost as many crystal-growing techniques as crystals. Certain factors, however, are basic to them all. The factor commonly accepted as most important is the rate of heat removal from the growing crystal face (17), which in

-18-

turn depends on the rate of heat loss from the solid and heat gain from the liquid.

It is generally believed (18) that atoms can enter into an orderly lattice arrangement much faster than common rates of crystal growth allow. It might seem then that rates of growth should be increased, but if we examine the treatment of this question by Pfann (17) we find a limiting factor does exist. At the interface between solid and liquid the heat balance equation is given by:

$$\gamma_s G_s = RH + \gamma_1 G_1$$

heat leaving = heat arriving

$\gamma$ - thermal conductivity

G - temperature gradient

H - heat of fusion

R - growth rate

s - solid

1 - liquid

If the temperature gradient in the liquid were zero we would have maximum growth rate. This would necessitate the liquid being exactly at the melting point, or more specifically at the temperature of the interface if supercooling or impurities were present, a condition which would surely lead to excess nucleation and loss of single crystal character. Increasing $G_s$ would also increase R, but would most likely lead to induced thermal stresses and resulting defects in the crystal.

Pfann also suggests the use of the Peltier effect to cause cooling at the interface. For this to be effective, however, the Peltier coefficient for solid against liquid must be reasonably large and Joule heating must be small.

Excess nucleation in the melt upon cooling will result in a polycrystalline mass being formed instead of the desired single crystal. This danger increases as the extent of possible supercooling and solid impurity content increases. For these reasons extreme care must be taken to prevent the entrance of foreign bodies into the melt. The growth container and atmosphere are the usual sources of such contaminates. When single crystals are being grown from the melt by reaction of the elements and subsequent melting, the melt should be heated well above the melting point of the compound to facilitate complete reaction and destroy any nuclei. A large temperature gradient in the liquid helps reduce the degree of supercooling and thus reduces excess nucleation. Melt-grown crystals are also subjected to a zone-refining action as the interface slowly progresses. If little or no disturbance is present, as is certainly desired from a crystal growth point of view, an impurity-enriched zone with a higher freezing temperature may build up in the liquid at the interface. This effect which was pointed out by Rutter and Chalmers (19) and designated constitutional supercooling, may well lead to spurious nucleation. This phenomena must be taken into account when growing crystals with purposely added impurities. The presence of this layer can also lead to instability of the actual interface and hence to poor crystal formation. A comprehensive treatment of this problem is given by Wagner (20).

Some processes for melt-grown crystals employ the additional refinement of introducing a small seed crystal into the melt to obtain a more favorable orientation of the crystal. Certain crystal lattice types have preferred directions for growing, and single crystals can be produced more readily if growth is purposely started in one of these directions, particularly if the crystal is being grown in a comparatively narrow tube as if often the case. While the existence of these preferred growth directions has been clearly established (21), no extensive compilation of data has definitely shown that "allowing" the crystals to grow in these directions results in more perfect structures. Intuitively, it seems reasonable and Pfann suggests that available evidence indicates that it does.

Most materials which melt at reasonable temperatures without decomposition and are not too reactive can be grown from the melt. The general procedure is to cool one end of the melt until a seed crystal forms or purposely seed the melt and then pass a sharp temperature gradient through it to effect continued crystallization. Historically, Tammann (22) was the first to make extensive studies of procedures for growing metal crystals from the melt. He used a long narrow tip on the end of his crystal growing container, which he cooled until nucleation occurred, keeping the main melt slightly warmer. If several nuclei were formed at least one of them would have a favorable orientation to grow rapidly along the tube and "squeeze out" the other seeds by the time it reached the main tube. Further cooling of the remainder of the melt would often lead to one continuous single crystal. Bridgman (23) used the same idea, with the modification of cooling the tube to cause crystallization by lowering it into a heat sink,

usually air, the rate of travel being slow enough to allow for heat
removal and proper orientation of the advancing crystal front. The
usual container material was glass, but as higher melting crystals
were grown ceramic tubes came into use. Many specialized adaptations
of Bridgman's method were made for growing crystals of such materials
as nickel, copper, bismuth, and some alkali halides. A number of
special furnaces and lowering (or raising) devices were thus origina-
ted, but perhaps the most commonly used is that with which Stockbarger
(24) grew lithium fluoride crystals. The main feature of this tech-
nique is the use of a horizontally split vertical furnace. Each half
is independently heated and controlled with a platinum radiation
baffle between them. An extremely sharp temperature gradient can thus
be maintained which will cause crystallization as the melt is lowered
through it. Further refinements include exponential winding of the
heater wire at the ends of the furnace and a nichrome liner inside
the furnace to even out undesirable temperature gradients. Since
the bottom section of the furnace need be only slightly below the
crystal melting point there is no risk of thermal stresses being
incorporated into the growing crystal. For LiF, Stockbarger used a
double walled platinum foil crucible supported on an alumina cement
capped stainless steel lowering device. With this apparatus he was
able to produce LiF crystals up to three inches in diameter and
later modifications produced crystal six inches across of optical
quality.

A more usual growth process was that of Kapitza (5), who
grew metal crystals by the Bridgman method but was unable to obtain
the desired orientations. This he attributed to a difference in the

thermal expansion between the crystal, in this case bismuth, and the
container. To eliminate this he melted a rod of the metal on a shielded
copper plate and seeded the small end with a crystal of the proper
orientation. As the rod was cooled this orientation persisted through-
out the entire crystal. This same process is now employed in single
crystal growth by the zone refining technique.

A departure from these techniques is that of growing single
crystals without a container; that is, pulling the crystal from the
melt. The method was first used by Czochralski (26) to measure the
rate of crystallization of different metals, but was soon adopted to
produce single crystal wires. Briefly the process consists of plunging
a glass capillary into a melt of the metal and slowly withdrawing it.
Surface tension draws the liquid metal up to the capillary where it
solidifies and as the tube is raised a crystal grows down toward the
melt. Surface tension and the density of the metal will control the
allowable distance from the crystal face to the melt. As usual many
modifications were made of this method for different crystals, one
of the most recent being that of Roth and Taylor (27) for germanium
crystals.

A similar, but distinctly different method is that of
Kyropoulos (28) in which the crystal is grown from a seed actually
introduced into the melt. This method has been improved by Teal and
Little (29) and others for producing large germanium crystals and has
probably helped advance the technology of transistors more than any
other single technique. The entire melt can be pulled into the crys-
tal and by judicious additions of carefully selected "impurities"
during growth, junctions may be grown directly into the crystal. The

-23-

orientation of the seed crystal can be selected to produce the correctly oriented finished crystal, but apparently germanium grows equally well from several different faces (17). The seed crystal must be simultaneously, but independently, rotated as it is pulled from the melt. A rotation of about 100 rpm is usually sufficient to even out heat flow and maintain convection in the melt, while the pulling rate is generally in the region of 50 microns per second. A graphite crucible is commonly employed to hold the melt and act as a susceptor for induction heating. A complete treatment of the process of growing single crystals of germanium is given by Bradley (30).

Extremely pure crystals have been grown by this technique, the greatest causes of defects being thermal stresses, variations in growth rate and the presence of impurities. A zone leveling technique similar to that used by Kapitza can be applied to imperfect semiconductor crystals both to promote single crystal character and to level out impurity concentrations throughout the length of the crystal. This is particularly applicable to "doped" crystals where segregation may occur during growth.

A still different approach, particularly adaptable to stable refractory materials, is the flame fusion process developed by Verneuil (31). A fine powder of the material from which the crystal is to be grown is fed into the gas stream of an oxy-hydrogen burner before it reaches the burner nozzle. During combustion the powder melts and is carried by the flame to a rotation seed crystal cemented to a refractory rod. As more material is deposited on the seed and the crystal grows the support rod is gradually lowered.

## 3.3 Growth from Vapor Phase

Many of the more interesting semiconducting and photoconducting compounds cannot be crystallized from the melt because of a tendency to dissociate and vaporize. This is particularly true for many sulfides and selenides and some tellurides. Two general methods available to produce crystals of these materials are vapor phase growth and hydrothermal techniques, neither of which readily results in very large crystals. Heinz and Banks (32) have reported growing cadmium selenide single crystals in a pressure bomb at 1100 degrees C and 250 psi. These crystals, however, contained a large excess of cadmium.

The usual vapor phase process involves passing an inert gas over the molten constituents, carrying their vapors into a reaction chamber where the compound forms and crystallizes out on the walls of the chamber. Extremely pure, unstrained crystals can be produced this way although they are usually in the form of thin plates. Bishop and Liebson (33) have grown CdS crystals several square centimeters in area and up to one millimeter thick by this method, using argon as the carrying gas, and maintaining the reaction chamber at 1000 degrees C.

Frerichs (34) has grown CdS, CdSe, CdTe by reaction of cadmium vapor with $H_2S$, $H_2Se$, and $H_2Te$, respectively. Very pure single crystals in the form of thin plates a few $cm^2$ in area were obtained.

Small crystals of CdS have been obtained by simply placing a boat containing some CdS powder in a furnace with a temperature gradient present. Over a period of time some of the CdS will vaporize and condense in the form of crystals in a cooler part of the furnace.

## 3.4 Growth of Cadmium Telluride and Zinc Telluride

From a consideration of the previously discussed crystal growth processes and their properties it was anticipated that both CdTe and ZnTe could be best grown by the Stockbarger method. A modified stockbarger apparatus was constructed for this use; modified in the sense that instead of lowering the crystal, the furnace itself is raised thus eliminating possible vibrations from disturbing the growing crystal. A sectional diagram of the furnace is shown in figure 6. The heaters consists of 0.040 inch Pt-20% Rh wire wound uniformly on recrystallized alumina tubes except over the last two inches where an exponential winding was used. The radiation baffle is comprised of two thin alumina discs on each side of a two mil platinum foil giving a total thickness of slightly over 1/8 inch. Each side of the baffle is recessed to hold the alumina tubes in place and bring the two heaters closer together to give a sharper temperature gradient. The heater-baffle assembly is held in place in the stainless steel shell by insulating bricks, the remainder of the volume being filled with magnesia bubbles.

The furnace is mounted in the rack shown in figure 7, along with the power supply, temperature control units, and drive mechanisms. The furnace is counterweighted and mounted on rollers in tracks to facilitate movements up or down around the reaction tube. A lead screw mounted on the rack with brass bushings and running through a split nut on the side of the furnace can raise or lower the furnace by means of a gear train driven by a thyratron controlled variable speed motor. The rate of furnace travel can be regulated between 0.9 and 4 mm/hr., 15 inches being available for travel. The split nut can be opened and the furnace moved manually when desired.

FURNACE SECTION

Mg O Bubbles

K 30 Insulating Brick

$Al_2O_3$

$Al_2O_3$ Cement
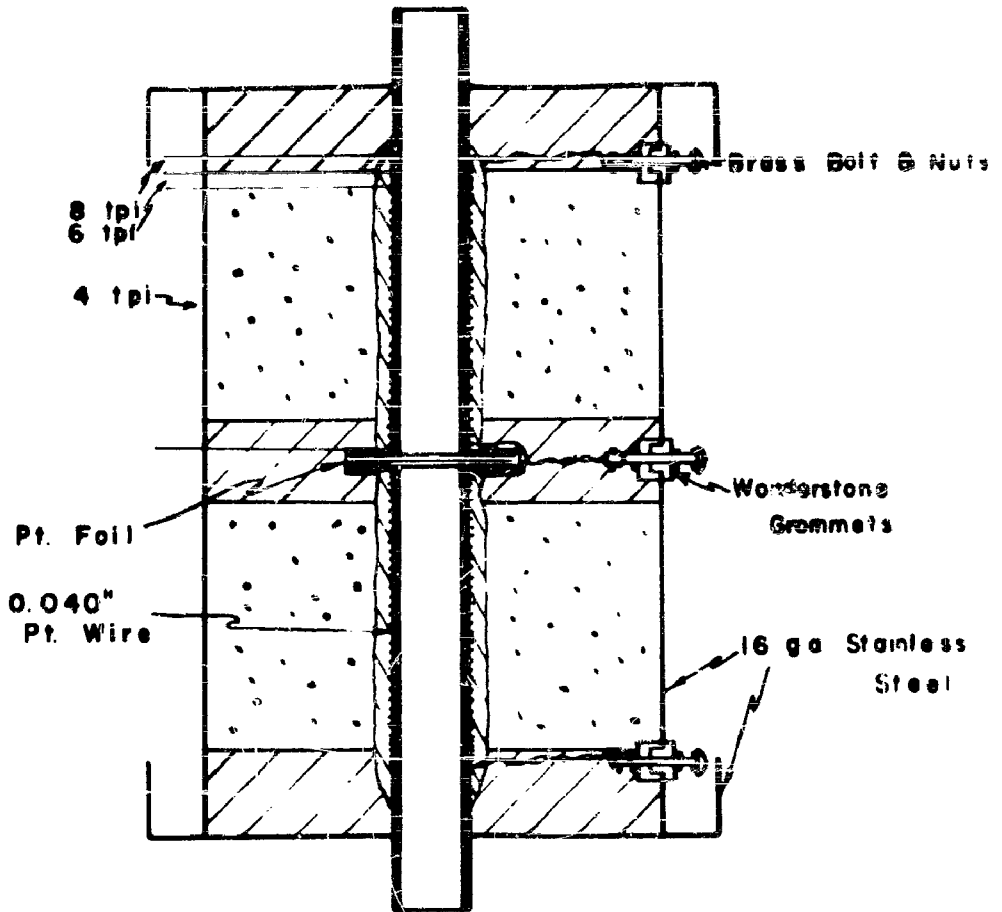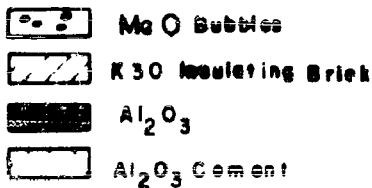
Scale  1/4" x 1"
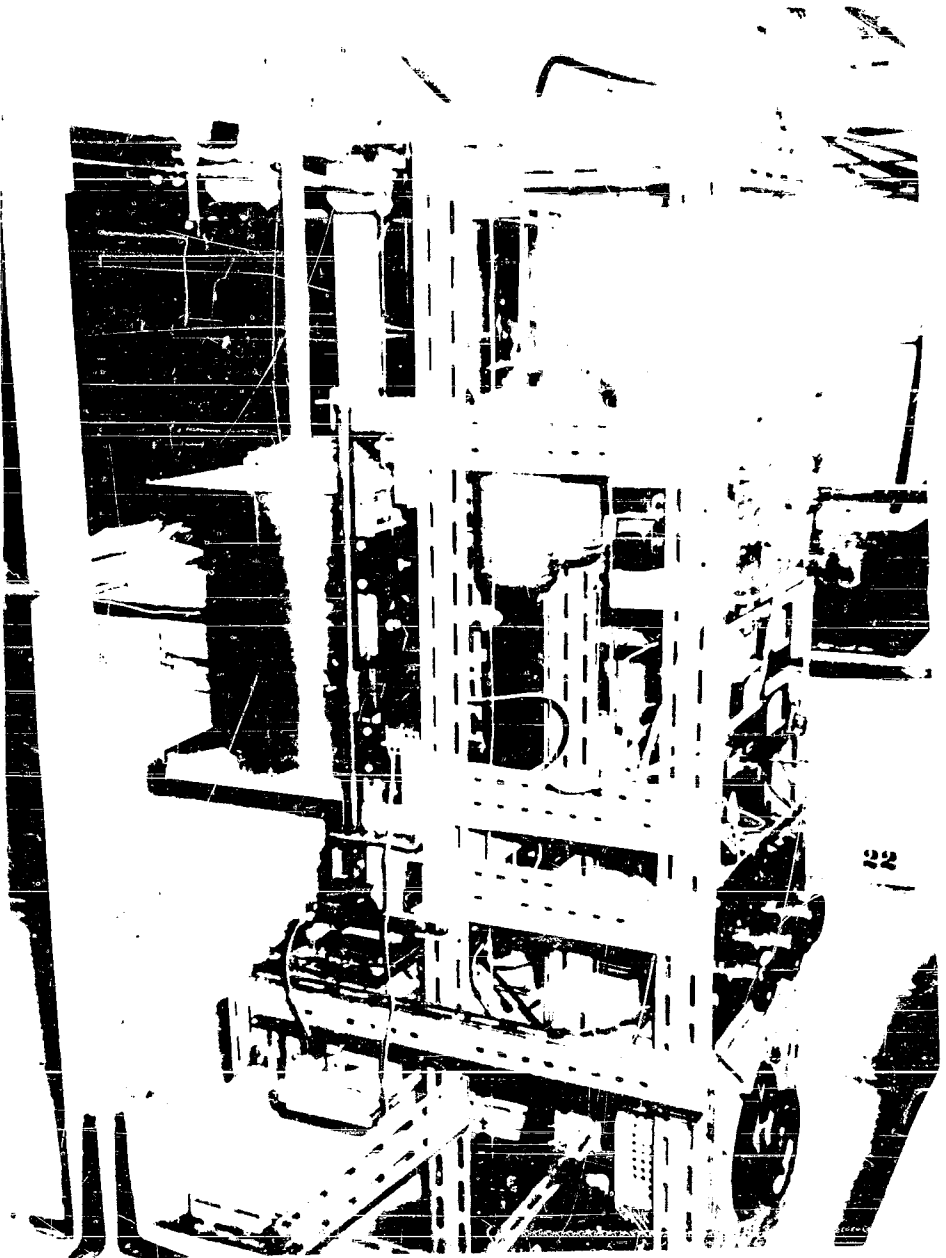
FIGURE  6

FIGURE 7

Power is supplied by a variable transformer, a variable power resistor being placed in series with the lower furnace winding to keep it at a lower temperature. Temperature control is of the incremental type; that is, the control units switch in and out of the circuit one side of a set of parallel resistors which is in series with the furnace winding. The degree of control is governed by the value of the two parallel resistors. For this furnace where each winding has about eight ohms resistance at operating temperature, one ohm resistors are used. Temperature control units themselves use platinum resistance thermometers imbedded in the furnace adjacent to the heaters as the sensing device. The control unit is given in figure 8 and consists of a Wheatstone bridge circuit operating at 60 cps, balanced by a ten-turn precision helipot. The bridge output due to changes in the resistance of the sensing device is amplified and fed to a phase splitting circuit feeding directly into a grid controlled rectifier which supplies the screen and control grid voltages of the beam power output tube. A Sunvic thermal relay with a capacity of 12 amps at 115 volts, which will switch with a current change of less than one ma from its normal operating position of about 20 ma is located in the plate circuit of the output tube. Short time control of about $\pm$ 0.1°C and overall control of about $\pm$ 0.5°C is attained with these units at 1000°C.

The furnace driving gear train is further reduced and extended to the transformer to give a rundown time of from 273 to 27.3 hours from full on. This allows annealing rates of from about 16 to 160 degrees per hour.

TEMPERATURE CONTROL UNIT

FIGURE 8)

The specimens were prepared for growth by weighing stoichio-metric amounts of zone refined tellurium and high purity cadmium into a thick walled silica container, 12 mm in diameter. These were then pumped down on a high vacuum system to a pressure of less than $10^{-6}$ mm of Hg and sealed off. The batch filled about 60 to 80% of the volume. This was then placed inside a mullite protection tube also connected to a vacuum system and suspended in the furnace, as shown in figure 7. Since CdTe melts at $1041^{\circ}C$ the container was heated to about $1120^{\circ}C$ and then cooled to $1080^{\circ}C$ before crystal growth was started to assure complete reaction and reduce the chance of any nuclei remaining. At this temperature the vapor pressure of CdTe is sufficient to cause the silica container to "balloon" out against the mullite tube. To prevent this it was found necessary to encase the silica tube in a close fitting alumina tube. The entire assembly is shown in figure 9.

Before starting to grow the crystal, the mullite tube was flushed several times with high purity helium to remove any oxygen which would diffuse through the silica at high temperatures, and to prevent contamination of the crystal in the event the silica container cracked. A slight overpressure was sealed off in the mullite tube to further help reduce the expansion of the container.

The furnace height was set manually so that the bottom of the container was about $1\frac{1}{2}$ inch above the baffle, assuring the entire tube of being at the same temperature. The furnace was heated at the rate of 100 degrees per hour up to $700^{\circ}C$. and 25-30 degrees per hour after that, since it is believed the highly exothermic reaction between Cd and Te takes place at about $770^{\circ}C$. The bottom furnace was brought to $1010^{\circ}C$ and the top to $1080^{\circ}C$ where the control units take over. It

was found advisable to hold the furnace at these temperatures overnight to assure thermal equilibrium throughout the furnace to permit the control units to be set for maximum sensitivity.

Furnace travel rates of from 1.5 to 6 mm/hr were used with no apparent difference in the quality of crystal grown. Two mm/hr was adopted as a standard, however, to eliminate any variables which did occur. Annealing rates were likewise varied with no appreciable effects. This also was standardized, at 25 degrees per hour. Using the standard technique described above, a success ratio of about 60% was obtained in growing single crystals of CdTe.

Since Jenny and Bube (5) had reported the occurrence of both n-type and p-type semiconductivity in impurity doped CdTe, melts were made containing 0.1 mole percent silver, bismuth, indium, antimony, and thallium along with pure CdTe. Those with Ag, Cu, In, and Sb proved quite successful, 30-40 gram single crystals being obtained. Thermal emf measurements indicate p-type character for Ag and Cu, and n-type for In and Sb. These results agree with what is to be expected from the normal substitutional feature of higher valence cations increasing the n-type character and lower valence cations increasing the p-type character. The opposite effect holds true for anion substitution, higher valence giving p-type and lower, n-type.

Pure CdTe turns out to be p-type, due probably to cadmium vacancies as has been suggested by Kroger and de Nobel (36).

A photograph of some cleaved pure crystals is shown in figure 10.

Powder method x-ray diffraction measurements of pure CdTe show the cubic unit cell parameter to be $6.457 \pm 0.005$ Å. Impurity
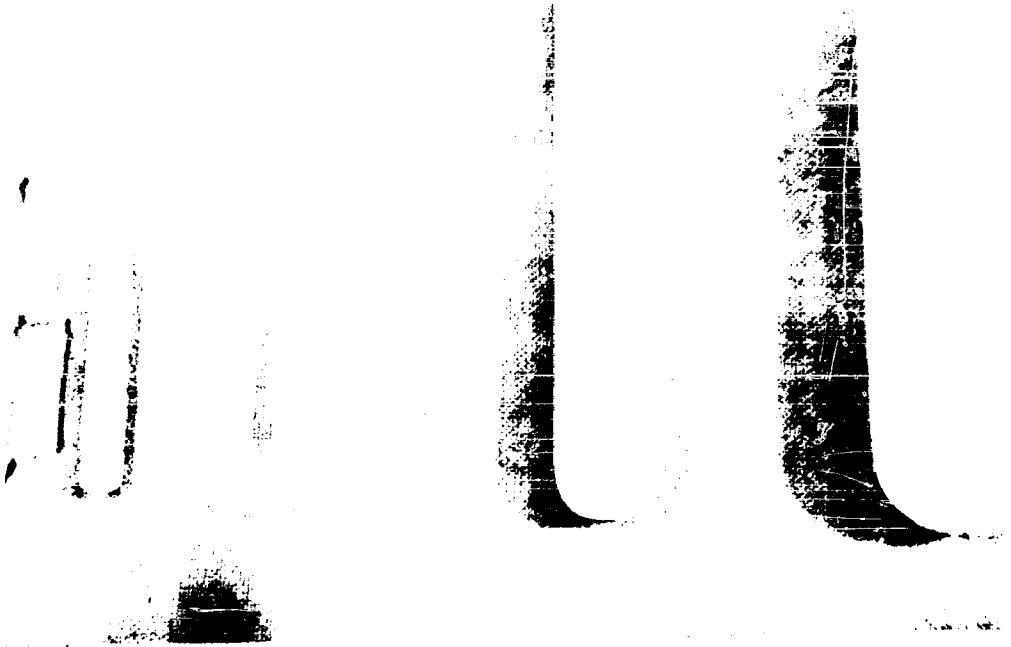
FIGURE 9
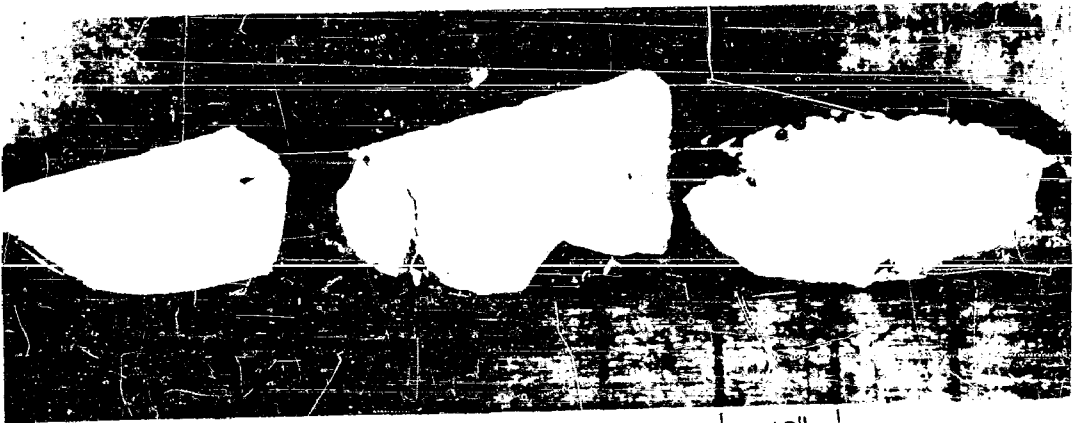


FIGURE 10          | 1/8" |

doped crystals were also investigated but no change in lattice para-
meter could be determined within these limits of accuracy.

Cadmium telluride crystallizes in the zincblende structure.
It always cleaves in the (110) plane and in this plane it cleaves
along the 111 direction.

Those batches which did not give single crystals wi all
complete polycrystalline masses indicating that extreme supercooling
may have taken place resulting in sudden crystallization when nuclei
did form. In no cases did a sample turn out to be single crystal
part way up the container and then degenerate into a polycrystalline
form.

Only one successful ZnTe single crystal was grown. The
higher melting point of this material (1280°C) seems to place it
at the extreme limit of this method. In practically all cases the
container broke, often violently. In an attempt to contain this
material a graphite die with a screw top was machined to enclose the
silica container. While no crystals were obtained using this arrange-
ment it was not investigated extensively and further adaptations,
mainly a substitute for the silica container, might well prove success-
ful. If so, it could be adapted to other volatile compounds such as
CdSe, and mercury selenide and tellurides.

## 4.1 Introduction

As of now, little will be said regarding the photoconductivity of a material, since it is closely related to its energy band structure. A brief review of the band theory will show how this is possible.

A solid is generally classified as a metal, semiconductor, or insulator depending on its electrical resistivity; metals having a resistivity in the region of $10^{-6}$ to ? ohm-cm, semiconductors say, $10^{-6}$ to $10^{10}$ ohm-cm, and insulators greater than $10^{14}$ ohm-cm. These divisions are somewhat arbitrary. The difference in conductivity arise from the differences in number of free electrons, free in the sense of being able to move through the crystal lattice and carry an electric current, metals having about $10^{22}$ free electrons per cm$^3$, or about one electron per atom and semiconductors and insulators having far fewer. The early Drude-Lorentz theory of metallic conduction treated the interior of the metal as a region of constant potential in which an electron "gas" flowed, resistance arising as a result of electron collisions with the metal ions forming the lattice. The resistance of such conductors increases with increasing temperature because of an increase in the vibrations of these metal ions. Band theory, however, assigned a system of waves to the moving electrons which describe the motion of the electrons and have a wavelength

$$\lambda = \frac{h}{mv} \tag{1}$$

where h is Planck's constant, m is electron mass, and v is the velocity of the electron.

The kinetic energy of the electron is given by

$$K.E. = \frac{1}{2} mv^2 \qquad (2)$$

but since from (1)

$$v = \frac{h}{m\lambda}$$

$$K.E. = \frac{h^2}{m\lambda^2} \qquad (3)$$

and so an energy vs reciprocal wavelength plot is parabolic (figure 11).
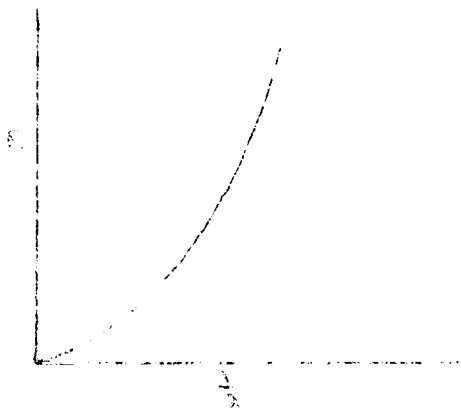


Figure 11

Calculations of permitted velocities of electrons in this metal using the Schrodinger wave equation with a constant potential show a series of velocities corresponding to definite wavelengths according to equation (1). This means the electron is permitted only certain discrete velocities (energies), and so figure 11 should more accurately be represented by a series of closely spaced dots, corresponding to this series.

Since there are more possible energy levels in a crystal than there are electrons, if we start filling the levels, making use of the Pauli exclusion principle, which states that two electrons may occupy

the same level only if they have opposite spins, so that all the levels

up to some energy will be filled and those above that level empty at

$T = 0^0K$. At higher temperatures there will be a statistical distribution

of filled states above this energy and empty ones below it. These upper-

most electrons have to be essentially free, only a small energy being

needed to raise them up to empty levels where they may conduct.

The differentiation between conductors and non-conductors can

be explained on the basis of overlapping and partially filled zones.

Figure 12 demonstrates two possible cases where the energy E is plotted

against $N(E)$. $N(E)$ represents the number of states in the energy range

E to $E + \Delta E$.



|  |  |
|---|---|
| $N(E)$ | $N(E)$ |
| 12a | 12r |
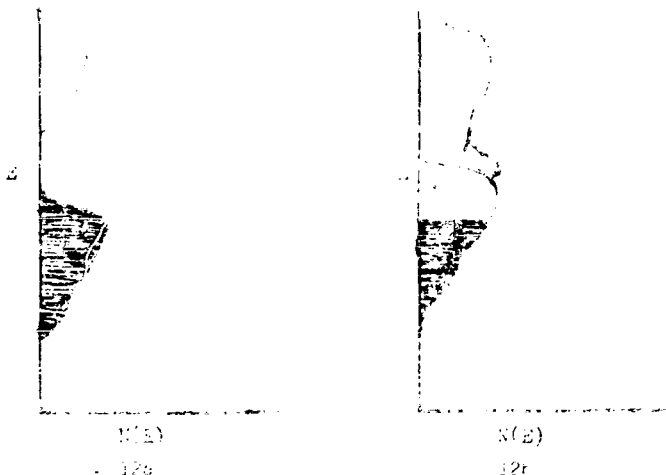
Figure 12

In 12a the first zone is completely full and the second zone is empty.

There is, moreover, a region of forbidden energies separating these zones.

An energy greater than this gap must be supplied the electrons before

they can be raised to an empty level in which they are "free". If, on the

other hand, the bottom zone were not completely full, the uppermost electrons

-33-

would have a continuum of states to which they could easily be raised
and contribute to a conduction process. In (2) the zones overlap so
there is also a continuum of possible energy levels to which electrons
may be easily raised. Covalent, and particularly ionic crystals gener-
ally have narrow zones and large gaps because of their varying potential
field and since each atom or ion supplies an even number of valence
electrons, the highest filled zone will be completely full. These
materials then will not exhibit metallic conduction. They may be made
to conduct only if sufficient energy is supplied to some electrons to
raise them across this gap. If a sufficient concentration of free elec-
trons and holes is created by thermal excitation to give rise to a resis-
tivity in the range $10^{-2}$ to $10^{10}$ ohm-cm the material is called an intrinsic
semiconductor. The number of electrons in the conduction band of a semi-
conductor or insulator with energy gap E and at temperature T is:

$$n = n_0 e^{-E/kT}$$

where k is the Boltzmann constant.

At room temperature $kT \approx 0.025$ eV, so for diamond for which $E \approx 10$ eV

$$n = n_0 e^{-400}$$

which will be an extremely small number of free electrons.

For grey tin, $E \approx 0.1$ eV so

$$n = n_0 e^{-4}$$

which means that about one percent of the states in the conduction band
will be filled.

Thus, we see that there is no real difference between insulators
and semiconductors, the designation depending only on the width of the
forbidden zone. If the conduction process is due to free carriers arising
from discrete levels located in the forbidden zone the solid is said to

exhibit extrinsic semiconductivity. Two types of such levels are possible; donor levels which normally are the electrons which may be "donated" to the conduction band, and acceptor levels which may "accept" electrons from the valence band giving rise to free holes. As one would anticipate, semiconductors and insulators generally have a negative thermal resistivity coefficient, the resistance decreasing as the temperature increased due to the increase in the number of free current carriers with temperature.

In solids with impurity levels, however, there may be a temperature range between the extrinsic and intrinsic conductivity regions in which a positive thermal resistivity coefficient exists. This arises from the fact that the impurity levels, which will be ionized at low temperatures, may be emptied before intrinsic conductivity assumes full control of the conduction process. In this state the material is similar to a metallic conductor.

If energy is now supplied to the solid sufficient to change the number of free carriers, a change in conductivity will be occasioned. If this energy is precisely defined, the gap width or the distance between various levels in the forbidden zone and the valence and conduction bands may be determined by noting the energies which cause the greatest increases in conductivity. Since the maximum intrinsic energy gap width usually encountered in semiconductors is of the order of 2.5 eV, one of the most convenient methods of supplying this energy is optical radiation.

The quantum relation $eV = h\nu$ , where $e$ is electron charge, $V$ is volts, $h$ is Planck's constant, and $\nu$ is frequency of the radiation, shows us that radiation of wavelength 12396 Å will have an energy of 1 eV. From this we see that radiation of wavelength 5000 Å corresponds to 2.5 eV. Shorter wavelengths would supply higher energy and so actually semiconductors and insulators both may exhibit photoconductivity, but since the

occurrence of photoconductivity in insulators such as the alkali halides is generally treated differently than in semiconductors, we will concern ourselves mainly with semiconductors.

As was stated previously, much of the earlier work on photoconductivity was done in insulators by Gudden and Pohl (37). They distinguished between two types of photoconducting crystals; those characterized by high index of refraction ($>$ 2) whose properties were dependent on the material itself and not induced by defects, and those whose photoconductivity arose from induced defects, the pure solid showing no photoconductivity. The first type is exemplified by diamond, while colored rock salt is the classic example of the latter. They also distinguished between primary and secondary currents and list the following characteristics.

| Primary | Secondary |
|---|---|
| Instantaneous rise time | Slow rise time |
| Small temperature dependence | Large temperature dependence |
| Unit quantum efficiency | Quantum efficiency greater than unity |
| Occurs in perfect crystals | Usually occurs in impure crystals |
| Proportional to light intensity | Hysteresis effects often occur |
| Current proportional to field, saturates at high voltages | No simple relation to applied voltages |

Since the primary current makes up the actual photo effect, it is best studied in "perfect" single crystals. The secondary current, because of its greater quantum efficiency, is generally considered to be due to a lowering of barriers in the material, and so it is best examined in polycrystalline films.

The early work on photoconductivity in semiconductors did not take the difference between primary and secondary photocurrents into account and since natural crystals of unknown purity were used the results are not too reliable. Sudden and Pohl did find that long rise times due to secondary currents were present in CdS. They also showed the shape of the spectral response curve for HgS was altered depending on whether primary or secondary currents were present. Secondary current effects can be limited by use of pulsed or chopped light, and increasing the purity of the crystals.

As the significance of defect structure has become more apparent, present work has been directed more toward determining the location and nature of the discrete energy levels located in the forbidden gap, which arises from such defects as impurity ions, lattice vacancies, and dislocations. Since the "purest" of crystals, as prepared, will contain an ill-defined assortment of defects, levels are often purposely introduced by adding impurity ions or creating lattice vacancies to give a predominance of one type for investigation. Structural defects may occur in a variety of forms, such as cracks, and edge and spiral dislocations and so are much more difficult, if not impossible, to purposely introduce into the crystal in precisely defined amounts and types. Since the energy associated with these defects may give rise to energy levels in the forbidden gap, it is important to have as few of them as possible in the crystal so that their effects are not confused with effects due to purposely added defects.

These levels in the forbidden region will have lower activation energies than the intrinsic activation energy and so give rise to photo-conductivity effects in the infra-red. The spectral response of a photo-conductor then will depend on the intrinsic gap width and the location of

the energy levels in the forbidden gap. The actual magnitude of the photo-current, however, will depend on the lifetimes of the current carriers liberated.

If a photoconductor is subjected to optical radiation of energy equal to the intrinsic energy gap, free electrons will be raised to the conduction band and free holes will be created in the valence band. The lifetimes of these carriers will be determined by the recombination process occurring in the solid. Since each excitation cycle ends in recombination of an electron and hole at a discrete energy level in the forbidden zone, the concentration and capture cross section of these levels for electrons and holes will control the recombination process and hence the photoconductivity.

The most detailed semi-quantitative account of recombination processes is that due to Rose (38), which more recently has been put on a quantitative basis by Bube (39) in accounting for the photoconductive properties of CdS type photoconductors (CdS and CdSe). A review of this treatment is presented here with a view to accounting for the photoconductivity of CdTe on a similar basis.

The three main observations for which suitable recombination pictures are not available are (1) "supralinearity", that is photocurrent which increases with a power of light intensity greater than unity, (2) increase in photocurrent with the addition of recombination centers, and (3) "infra-red quenching", decreasing the photocurrent due to short wave-length radiation by the addition of long wavelength radiation.

While many simple models are often available to describe some semiconductivity observations, it is difficult to propose even one for the phenomenon of "supralinearity". The second observation seems in-tuitively unlikely and the third has been reported both in semiconductors

and insulators, usually applied to luminescence but also to photoconductors, and even electroluminescence (40). As will be shown later, two different types of recombination centers with different capture cross sections for electrons and holes are necessary in any single model which can account for all these effects.

It is generally accepted that transitions do not take place directly between the discrete energy levels in the forbidden zone at low densities of states, although such transitions may well occur if the density of states exceeds about $10^{17}/cm^3$. These states are further pictured as having a capacity of either one electron or hole and are considered to be the sites of carrier capture, which for the sake of simplicity and lack of evidence to the contrary is considered as a one step process. At equilibrium, under radiation of energy equal to the intrinsic energy gap, electrons and holes will be combining at these levels at the same rate they are being generated.

Consider now the energy level model given in Figure 13 showing the possible array of possible states and their statistical division. The Fermi level is defined as the energy at which the probability of a state being filled is one half, and for intrinsic semiconductivity this level will be exactly in the middle of the forbidden gap if the effective masses of electrons and holes are equal. The steady state Fermi level for electrons (holes) is a mathematical concept introduced to describe the concentration of free electrons (holes) and is located at that energy where half the donor (acceptor) levels are occupied.

S.S.F.L.
(electrons)

F.L.

S.S.F.L.
(holes)
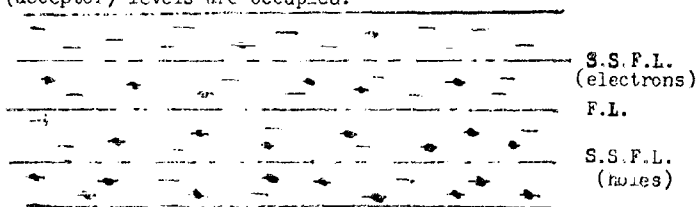
Figure 13
-39-

These states nearest the edges of the valence and conduction
bands are designated as shallow trapping states because they are essen-
tially in thermal equilibrium with the valence and conduction bands; those
nearest the center are ground states where recombination takes place.   It
should be mentioned here that the concept of traps is statistical in nature
and merely indicates a higher probability for electrons to be thermally
excited out the top of the trap than to fall through the bottom by recom-
bination with a hole.  Electrons and holes falling into ground states are
considered to have completed their excitation cycle.  While it appears
intuitive that shallow traps should exist the question of where to draw
the line between them and recombination centers may arise.  If there is a
reasonably uniform distribution of discrete states in the forbidden zone,
the demarcation line is drawn at that energy at which an electron is equally
likely to be captured or thermally excited into the conduction band, like-
wise for holes.  To a first approximation these lines correspond to the
steady state Fermi levels.  States between these steady state Fermi levels
will then be ground states and control recombination processes.  States
outside these levels will have a vanishingly small effect or recombination.

         If the solid is subjected to an excitation process which causes
an increase in the number of free current carriers (both holes and electrons)
the steady state Fermi levels will move outward toward the band edge and
some shallow traps will become ground states.  When the radiation is removed
the Fermi levels will approach each other and these ground states will re-
vert to shallow traps and be thermally emptied.

         The capture cross section of a center will generally have a
value of from $10^{-13}$ cm$^2$ down to smaller values with $10^{-22}$ cm$^2$ reported (41);
$10^{-15}$ cm$^2$ being a common value which corresponds to the approximate size
of a lattice site.  Different capture cross section for electrons and holes

are likely to be displayed by any particular level. A positively charged center, for example, will have a greater cross section for capturing an electron than a hole and similarly a negatively charged site will be more likely to capture a hole. Capture cross sections for electrons of $10^{-21}$ $cm^2$ have been found in CdS (12) while the capture cross section of these same states for holes is of the order of $10^{-14}$ $cm^2$.

The first actual case to be considered is that of an insulator or semiconductor with one class of discrete energy levels, in which there are several possibilities, including those where (1) carrier concentrations are small compared with ground state concentrations, (2) carrier concentrations are large compared with ground state concentrations, and (3) carrier concentrations are intermixed with ground state concentrations. Following these are those cases which include the addition of shallow traps and a continuum of discrete energy levels.

(1) The usual case for a photoconductor is that in which the concentration of free carriers, n and p, is small compared to their concentration in ground states, a condition arising from low excitation intensity. This case is shown in figure 14a where a solid with a set of ground states located near the Fermi level is undergoing an excitation process. At equilibrium, electrons must be entering and leaving the conduction band at identical rates, and holes must be entering and leaving the valence band at the same rate. Since recombination occurs at the ground states, electrons and holes must be entering these levels at equal rates. The rate of excitation f $(cm^{-3}\ sec^{-1})$ is given by:

$$f = v\ s_n\ n\ p_g = v\ s_p\ p\ n_g \qquad (4)$$

where v is thermal velocity, $s_n$ and $s_p$ are the capture cross sections for electrons and holes, respectively.
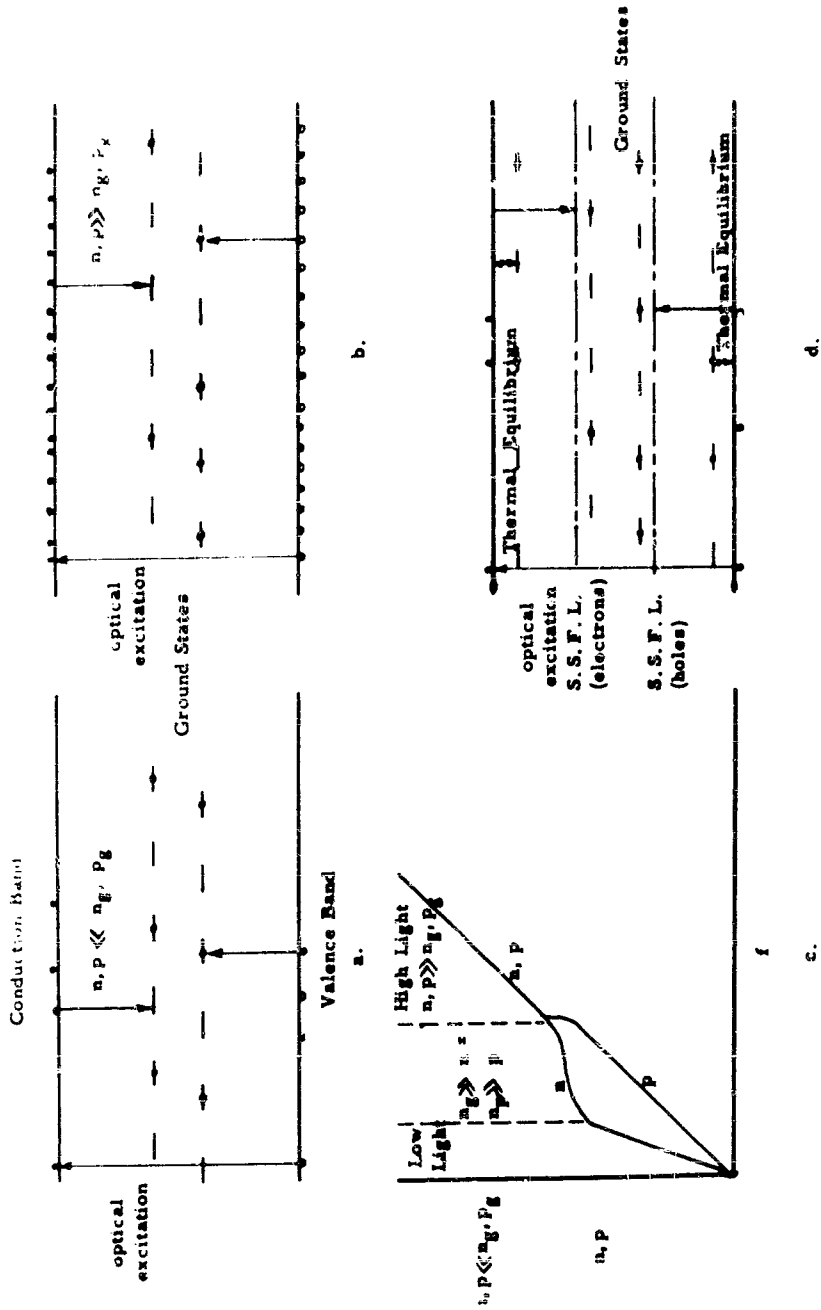
Fig. 14
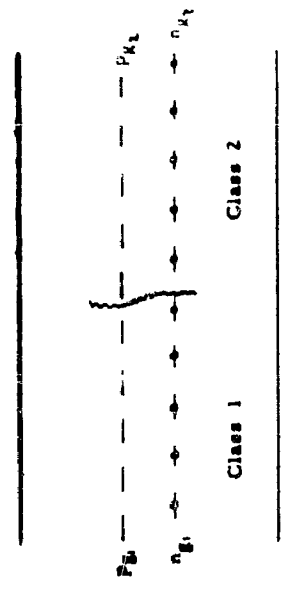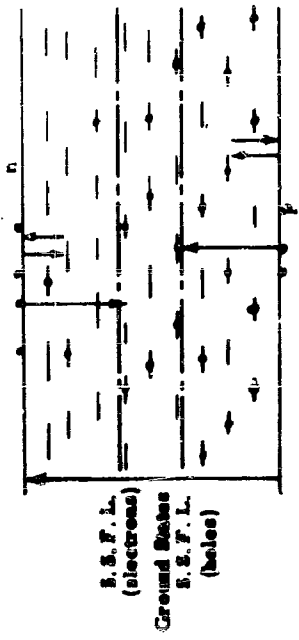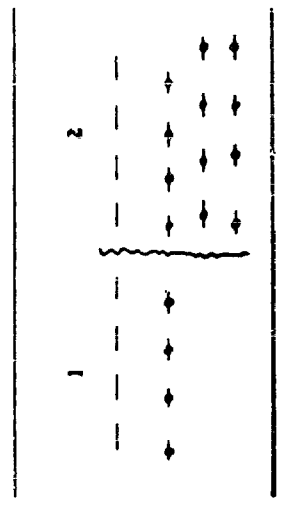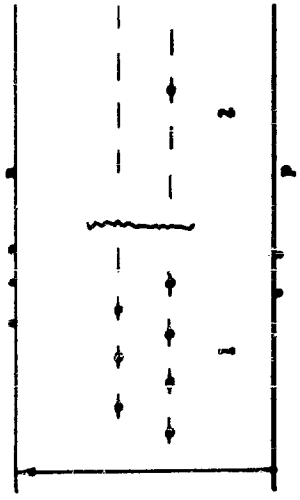
Since $n, p \ll n_g$, $p_g$, the concentration of electrons and holes in ground states after excitation will be approximately equal to their concentrations before excitation. Then $n_g$ and $p_g$ in equation (4) represent the concentration of electrons and holes in ground states before excitation, hence:

$$n = f/v \ s_n \ p_g \qquad \text{and} \qquad p = f/v \ s_p \ n_g \qquad (5)$$

n and p then being determined independently by capture cross section and ground state concentration. The lifetimes can now be given by:

$$\tau_e = 1/v \ s_n \ p_g \qquad \text{and} \qquad \tau_p = 1/v \ s_p \ n_g \qquad (6)$$

Free carrier concentrations then will increase linearly with excitation intensity. Although the concentration of electrons and holes in the ground states is the same after excitation as before, their distribution need not be the same. On the average, any given state will be occupied $n_g/n_g + p_g$ of the time by an electron and $p_g/n_g + p_g$ of the time by a hole.

The re-establishment of the original distribution may give rise to the long time decay tail in photoconductivity often observed. This process may also occasion the conductivity and luminescence "glo-curves" if the illumination is carried out at low enough temperatures to keep this re-ordering from taking place till the solid is warmed up.

Moss (43) gives the concentration of free photo-electrons for low light intensities as:

$$n = f/BM$$

where M is the concentration of recombination centers and B is a "recombination coefficient", with units of $cm^{+3}/sec$. Since n can always be small compared to M, and B is fixed, the photocurrent should always vary linearly with intensity at low intensities. The electron lifetime then is given by

$$\tau = 1/BM$$

Since B has the units of $cm^3/sec$, it can be seen on comparison to equation (6) to be equal to $v\ s_n$. If we take $s_n$ to be about $10^{-16}\ cm^2$ and $v \approx 10^7$ cm/sec, with a concentration of recombination centers, $N \approx 10^{16}\ cm^{-3}$, we get a lifetime of $\tau = 10^{-7}$ sec. Considering the widest likely limits for $s_n$ ($10^{-14}$ to $10^{-22}\ cm^2$) and N ($10^{11}$ to $10^{19}\ cm^{-3}$) we would expect lifetimes of from $10^4$ to $10^{-11}$ sec.

On the other hand, it is generally considered that minority carriers in insulating crystals are immobile, or nearly so, and have extremely short lifetimes. This view is supported by lack of transistor action in highly insulating crystals and general lack of p-type semiconductivity in such crystals (45).

While it is possible to measure majority carrier (electron) lifetimes by means of measuring photocurrent decay, it is necessary to use the photoelectromagnetic effect to measure hole lifetime. Following the work of Moss (44), it has been shown by Sommers and Berry (45) that holes lifetimes, as measured by the PEM effect, of at least $7 \times 10^{-7}$ sec can be found in CdS crystals of $p = 10^{10}$ ohm-cm where the electron lifetime is only $2.6 \times 10^{-6}$ sec. This existence of larger than predicted hole lifetimes had previously been suggested by Smith (46).

(2) In the case where $n, p \gg n_g, p_g$, (figure 14b), the concentration of free electrons and holes at equilibrium under high intensity excitation will be approximately equal, although their ground state concentrations after illumination do not have to remain equal to their concentrations prior to illumination. Since free holes and electrons are being generated at equal rates their lifetimes will be equal. Therefore

$$1/v\ s_n\ p_g = 1/v\ s_p\ n_g$$

and
$$n_f = s_n N_f / s_n + s_p, \quad p_f = s_p N_f / s_n + s_p$$

where $N_f = n_f + p_f$

Their common lifetime then is

$$\tau = \frac{1}{n N_f \dfrac{s_n s_p}{s_n + s_p}}$$

From this the electron and hole concentration is given by:

$$n = p = \frac{f}{r N_f \dfrac{s_n s_p}{s_n + s_p}}$$

which as in the previous case is linearly proportional to excitation intensity.

(3) When free carrier concentrations are intermixed with ground state concentrations, that is, when either $n_f \gg n \approx p_f \gg p$, or $p_g \gg p \approx n_f \gg n$, we have the case arising from medium radiation intensity. Taking the first case, from previous arguments $n_g$ remains constant and $p_f$ will remain $\approx n$ under illumination so

$$n = f/v \, s_n \, n = (f/v \, s_n)^{\frac{1}{2}}$$

The electron lifetime will now depend on their concentration and so the concentration of free electrons will increase only as the square root of the radiation intensity.

Again considering the case of only electron carriers, Moss arrives at a one-half power equation at higher radiation intensities when the concentration of free electrons becomes much larger than the concentration of recombination centers. Smith (47) has shown that a linear relation between photocurrent and light intensity holds for CdS over several orders of magnitude, but decreases to a one-half power relation at higher intensities.

These three cases are graphically summarized in figure 14c. The particular shape of these curves naturally depends on the values of $s_n$, $s_p$, $n_f$, and $p_f$. The above figure corresponds roughly to the situation $s_n \ll s_p$, and $n_f \gg p_f$.

Figure 14d represents the band picture with the addition of shallow traps. The addition of these traps will serve mainly to increase the rise (and decay) time of the photocurrent since more free current carriers must be produced. The rise (decay) time then will be increased by the **ratio** of trapped to free carriers. At high radiation intensities, of course, these shallow traps may become ground states, in which case the discussion is the same as (2).

In order to explain the fractional power increase of photocurrent with intensity and the rapid increase in response speed with light intensity, the model shown in figure 14e is proposed. The increase of photocurrent as a fractional power of intensity is explained on the basis of a decrease in the lifetime of the free carriers as radiation intensity increases. This occurs as a result of an increase in the number of states, which will have a high probability of acting as recombination centers, brought about by the separation of the steady state Fermi levels.

Response time is given by $\propto (n_t/n)$ where $(n_t/n)$ is the ratio of trapped to free carriers. n will increase almost proportionally with light intensity and since $n_t$ will remain almost constant and $\propto$ decrease but slowly, the response time can decrease at almost the same rate as n increases.

This complex model, although satisfactory for the preceeding considerations, will still not adequately explain supralinearity, infrared quenching, and activation. For these, the addition of another class of levels is required (figure 14f).

-45-

With the addition of these, the phenomena of activation can be accounted for on the basis of one of the classes of states having a different capture cross section for electrons than for holes. If for one class of states (I), the capture cross section for electrons and holes are the same and for the other class (II), the capture cross section is much less for electrons than for holes, then under low excitation (free carrier concentration small compared to ground state concentration) the state with similar capture cross sections will gradually become saturated with electrons since the other class of states has little tendency to capture electrons, so electron lifetimes will increase. This situation is given in figure 14g. The "latent" periods observed by Frerichs (48) in CdS are proposed to be due to this redistribution of electrons from one class to the other. This period consists of a time interval after initiating illumination on a crystal which had been in the dark for a long period, before the photocurrent rises rapidly to its equilibrium value, appearing as if the radiation is activating the crystal.

Infra-red radiation applied simultaneously with short wavelength radiation tends to raise electrons up to the empty class II states allowing holes to be captured in the class I states which are full of electrons, thus helping to reestablish the original distribution and thereby decreasing or quenching, the sensitivity.

If the class II states are spread over a wider region in the forbidden zone than the class I states (figure 14h), as the intensity of radiation is increased, more of them will function as ground states (the steady state Fermi levels will be moving apart). The class I states will become more and more filled, thus steadily increasing the lifetime of the free electrons. This results in increasingly sensitive photoconductivity and so supralinearity occurs.

At sufficiently high radiation intensities, however, the concentrations of free electrons and holes will greatly exceed the concentration of ground states, and become equal to each other. Effects due to the ground states then become negligible and the photoconductor is no longer sensitized by their presence.

Rose also gives an account of recombination in semiconductors which apparently applies only to extrinsic semiconductors, in which there is a greater concentration of one type thermally produced carrier than the other. An analysis of the free carrier lifetimes at low and high excitations in this solid leads to the conclusion that with only one type of ground state a supralinear photocurrent vs intensity plot can be obtained.

If more than one class of ground state is present, high intensity radiation will give shorter lifetimes because of the increase in the number of recombination centers. Low intensity radiation can result in a variety of effects. The lifetimes of both carriers may be shortened or lengthened depending on the various concentrations and distributions of free carriers and ground states.

Rose summarizes by listing four parameters and their possible values by means of which various recombination processes may be described, these being:

| | |
|---|---|
| material: | insulator, semiconductor |
| excitation range: | low, intermediate, high |
| ground states: | one class, more than one class |
| lifetime: | electron, hole, free pair |

Bube (39) has applied these theoretical considerations to CdS and CdSe and arrived at the band picture for these photoconductors, on a more mathematical basis. A model containing two classes of recombination centers filled in the dark and a set of trapping levels normally empty in

the dark is necessary to describe supralinearity, temperature dependence, infra-red quenching, and speed of response.

The levels associated with supralinearity occur at 0.64 eV and 1.0 eV above the valence band in CdSe and CdS, respectively, with a ratio for the capture cross section of holes to that for electrons of $3 \times 10^5$ for CdSe. Since supralinearity occurs in "pure" crystals of these compounds, it appears as if these levels are associated with a lattice defect, probably cation vacancies.

In investigating luminescence effects in silver-activated CdS, Lambe and Klick (47) also arrive at a model containing two different levels in the forbidden gap, which they designate quenching centers and activator, or luminescence, levels. Both of the centers act as recombination centers using it se's definition of the term although they refer to them as traps. The activator levels (due to Ag ions) lie about 0.4 eV below the conduction band and have a large capture cross section for holes: this capture giving rise to luminescence. Once a center has captured a hole it cannot contribute further to luminescence until it has captured an electron to recombine with the hole, thus returning the level to its original state. This step may take much longer than hole capture and so can account for the much longer decay of photoconductivity and the rapid decay of luminescence, when radiation is removed.

The quenching centers are those empty levels normally found in CdS at 1.0 eV above the valence band and have supposedly near equal capture cross sections. Their function is to provide free holes which stimulate luminescence and consequently quench photoconductivity when illuminated with 1.0 eV radiation. These levels correspond to those found by Bube (39) at 1.0 eV above the valence band in CdS and 0.64 eV above the valence band in CdSe, which he finds to have much larger capture cross sections for holes

-48-

than electrons. The ratio of capture cross section for holes to that for electrons for CdS is given as 4 x 10³. As will be shown later, photoconductivity measurements made on pure CdTe can be explained on the basis of equal capture cross section for electrons and holes for the corresponding levels 0.6 eV above the valence band.

Kenan, working by Halsted (40) on ZnCdS type, (3) phosphors, which had an alternating electric field applied parallel to the radiation, using one transparent electrode, have shown that luminescence is strongly dependent upon instantaneous free electron density in the irradiated surface. These observations appear to be in substantial disagreement with the above Lambe Klick model.

It should be noted here that many two center types of recombination processes are possible and as Bube (41) has shown a nonlinear rise of photocurrent and luminescence with radiation intensity can be explained by at least two different center models. Any model which is illuminated with radiation equal in energy to the fundamental energy gap can show a rise in photocurrent or luminescence which increases with a 0, $1/2$, $2/3$, 1, $3/2$, ... or $\infty$ power of radiation intensity.

While CdS has been extensively investigated for some time (42, 43) it has been only in the last few years that CdSe and particularly CdTe have received appreciable attention, due in part to the lack of precisely defined crystals of these materials. Frerichs (34) in working on phosphors grew single crystals of CdTe along with CdS and CdSe and found them to show photoconductivity although they were not phosphorescent. They were sensitive to all radiation from infra-red to ultra-violet, x-rays, gamma rays, and alpha and beta particles. Two types of photoconductivity were found to occur; normal photocurrent in the region of strong absorption from blue to ultra-violet and selective photoconductivity

in the region of weak absorption, from visible, x-ray and particle radiation.

The semiconducting properties of CdTe were investigated by Appel [52] who found four thermal activation energies in the temperature range from room temperature to 1150°K (1.5 eV, ...... 1.45 eV, 1100-950°K, 0.47 eV, 900-700°K, 1.45 eV, 700 ...350°K). Since CdTe melts at 1371°K and has been shown [53] to lose Cd above .... 900°C, the high temperature values, which are not for a stoichiometry, may be anomalous, at least as for as indicating band structure.

Transmission measurements [54] of CdS, CdSe, and CdTe indicate activation energies of 2.42 eV for CdS, 1.74 eV for CdSe, and 1.4 eV for CdTe. The difference in the adsorption wavelengths has earlier been reported by Noguich and Kompe [55] to be due to the differences in lattice dimensions.

The shift of these activation energies with temperature was measured by determining the shift in wavelength giving greatest photocurrent [56]. The photosensitivity maxima of CdS and CdSe showed structure indicating the possibility of double conduction or valence bands. No such structure was evident with CdTe, but radiation wavelength extended to only slightly past one micron. The shift in the activation energy and wavelength maximum were found to be:

$$e = 1.52 - 0.00060T \text{ eV}$$

$$\lambda = 8110 + 2.85T \text{ Å}$$

Van Doorn and de Notel [57] irradiated single crystals of CdTe and biased CdTe p-n junctions in the forward direction, both of which led to luminescence with a wavelength maximum at 8870 Å. They found the shift in activation energy to vary with temperature, having a value of $2.34 \times 10^{-4}$ eV/°K at 77°K and $5.15 \times 10^{-4}$ eV/°K at 600°K. They also found levels in the forbidden band at 0.2 eV and 0.15 eV from the valence

band due to $n_i$ or $d_i$ ... ... ... vacancies, and levels $0.... .V$ from the conduction band due to In ... or Te vacancies.

## 4.2 Apparatus and Measurement

a. Sample Preparation: Samples were prepared for measurement by cutting suitably sized specimens from the single crystal as taken from the furnace. The cutting operation was performed either by an "airbrasive" unit or a water-cooled carborundum disk rotating at 10,000 rpm, followed by removal of the surface layer with the "airbrasive". The "airbrasive" consists of a stream of fine fused alumina particles carried by a high pressure dry nitrogen gas jet, thus giving a cool cutting action, not likely to introduce surface defects from localized heating, although some mechanically induced defects are no doubt possible. For thicker samples, however, the nitrogen jet disperses so greatly it is difficult to cut accurate geometric shapes and so the carborundum disk is used. Although it is water cooled, localized heating certainly occurs at the blade edge. Removal of the cut surface to a depth of one-half millimeter by the "air-brasive" is considered adequate to remove any effects due to this heating. Samples were always cut to a finished size of either $2 \times 4 \times 8$ mm$^3$ or $2 \times 3 \times 6$ mm$^3$.

The theoretical aspects of forming noise-free, ohmic contacts to semiconductors based mainly on work functions has been treated by Smith (56), Kroger (57) et al. Indium and gallium were reported (56) to perform best on CdS (n-type). Bube and Jenny (35) used electroplated nickel and copper on both n- and p-type CdTe to which the leads were soldered. The use of In on n-type and Au on p-type CdTe is reported by Kroger and de Nobel (35). This was the scheme adapted for this investigation with the exception that In was used on pure CdTe for reasons which will be explained later.

Typical n-type crystals (In impurity) with In contacts have resistances in the range 2500 ohms whereas gold contacts give the same specimens apparent resistances of 100-200 K ohms. Typical p-type samples (Ag impurity) with gold contacts have resistances of $10^4$-$10^5$ ohms while the same specimens with In electrodes show apparent resistances of 1 - 10 x $10^6$ ohms. A pure crystal of CdTe, which would be p-type due to cadmium vacancies, gave an apparent resistance of $9 \times 10^7$ ohms with In contacts and after these were removed with the "airbrasive" and Au applied the apparent resistance dropped to $8 \times 10^6$ ohms.

The indium electrodes are applied by vacuum plating. Since molten indium will not "wet" a tungsten heating element it is evaporated from a conical silica boat supported in a helix shaped tungsten wire heater. The crystals are suspended by fine platinum wires 3 to 4 inches above the boat, the entire assembly being enclosed in a bell jar kept at a pressure of $10^{-6}$ mm Hg by continual pumping by a mercury diffusion pump.

Since electrodes are desired only on opposite ends of the samples the remaining sides are carefully cleaned off with the "airbrasive" unit.

Gold contacts are applied by touching a drop of $AuCl_3$ solution onto the desired spot. The solution is allowed to remain there a few seconds and then blotted off.

b. Thermal emf Measurements: To determine whether the samples are n- or p-type, the sign of the thermal emf was measured. A temperature differential of up to $80^{\circ}C$ was maintained across the crystal by pressing it between hollow copper blocks through one of which was flowing hot water and through the other cold water. The hot end will be nearer the intrinsic range than the cold so the Fermi level will fall in a n-type

-52-

material and rise in p-type. Since the Fermi level tends to remain level
the bands at the hot end of the crystal rise in an n-type crystal and fall
in a p-type. The hot end then will become positive for an n-type material
and negative for a p-type. These situations are shown in figures 15a and b,
respectively.
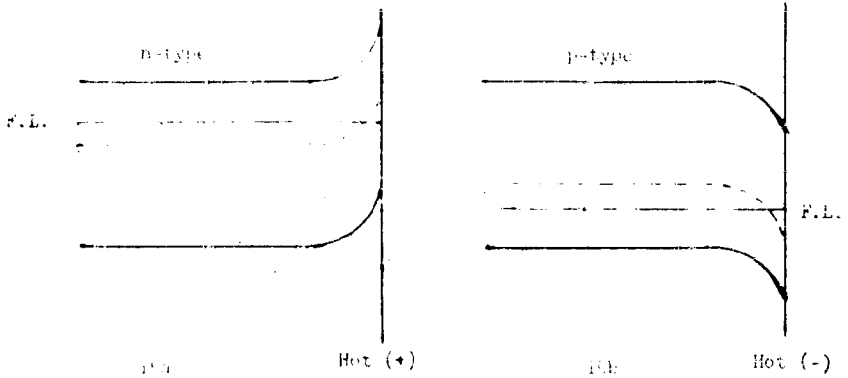


Figure 15

c. Thermal and Optical Measuring Equipment: All other measure-
ments were carried out in the sample holder described in figure 16, using
the measuring circuit of figure 17.
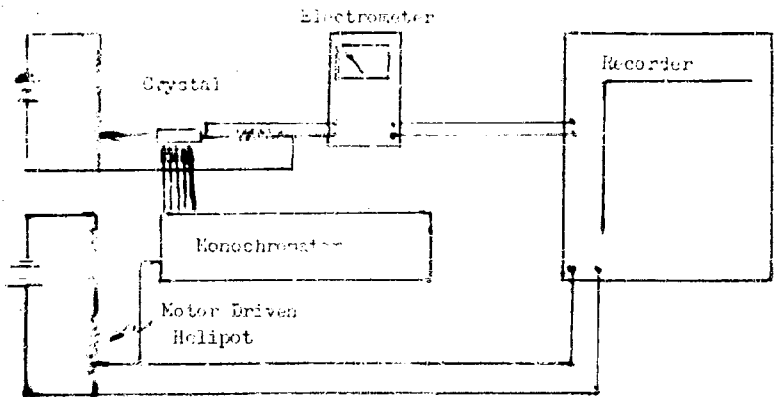


Figure 17
-53-
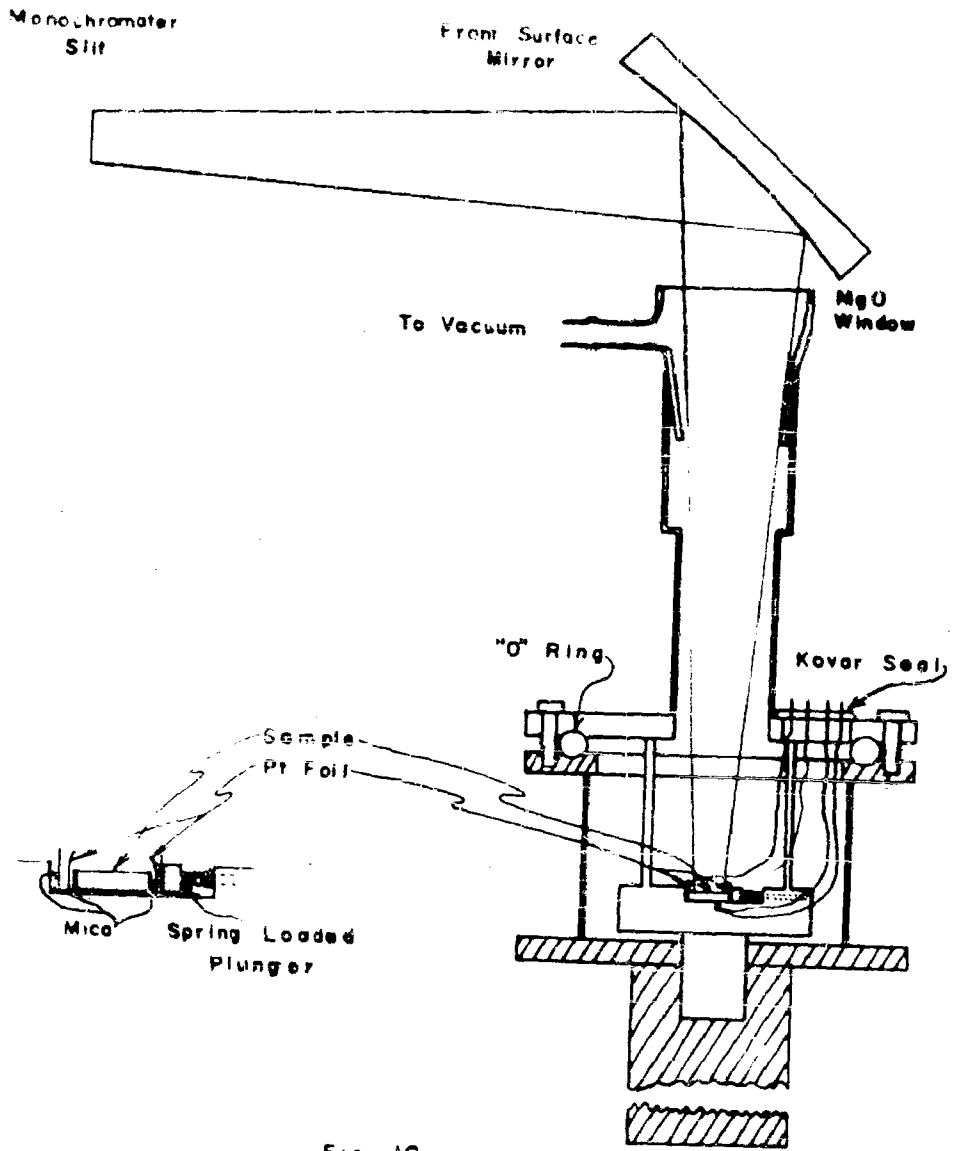
Fig. 16

A Perkin Elmer model 98 single-beam double-pass monochromator equipped with rock salt optics and a Glo-bar operated at $1600^{\circ}K$ is used as the radiation source covering the wavelength region of 0.5 to 15 microns. A ten-turn Helipot mounted on the wave drum of the monochromator in conjunction with a precision resistor and dry cell constitutes a voltage divider network feeding into the X axis of the recorder which is calibrated in terms of wavelength. The Y axis is fed directly from the current measuring electrometer circuit and is calibrated in terms of photocurrent. The current measuring circuit consists of a Keithly model 200B electrometer measuring the voltage drop across a decade resistance unit of one percent accuracy. This voltage is never more than 10 millivolts and since at least one volt is always used as the power source, the voltage of the power source will be the voltage across the crystal to an accuracy of at least one percent. Although only one volt was usually used across the crystal to avoid effects due to high fields, pure CdTe crystals have such high resistivities at low temperatures that up to 100 volts were used. The ratio of current under illumination to dark current was measured from one to 100 volts under standard conditions and little change was found.

The brass sample holder shown in figure 16 is attached rigidly to the monochromator, and connected to a vacuum and gas handling system. An atmosphere of high purity helium is maintained in the holder to facilitate heat transfer after it has been evacuated to a pressure of $10^{-6}$ mm. The sample is held in place by a spring loaded plunger which also presses platinum foil electrodes against it and is electrically insulated from the sample holder by 0.3 mm thick mica sheets. The foil electrodes are bent over the ends of the crystal to shield the contacts from the radiation. A thermocouple is imbedded in the holder adjacent to the sample for temperature measurement.

Sample illumination is accomplished through a periclase (MgO) window fused to the ground glass joint connecting the holder to the vacuum system. Samples may be changed without disturbing the position of the holder so that radiation conditions will be identical for all samples.

Since it is vital to have as nearly as possible identical ambient conditions with respect to the measuring equipment for each stage in a series of measurements, a dehumidified sheet aluminum enclosure was used to surround the entire apparatus. This gave much "cleaner" recordings and more uniform measuring conditions.

With this arrangement, photocurrents in the range of $10^{-5}$ to $5 \times 10^{-13}$ amps over the wavelength region of 0.5 to 9.5 (2.5 eV to 0.13 eV) can be measured and automatically recorded.

d. Impurity Doped Samples: The crystals doped with Ag, In and Cu were examined for signs of photoconductivity over the temperature range from room temperature down to $-196^{\circ}$C. Only one Cu impurity specimen (p-type) exhibited some photoconductivity below $-125^{\circ}$C in the region of 2 (figure 18). The absence of photoconductivity in the other impurity samples is almost certainly due to too great a concentration of impurity. This results in such low resistivities that any effect of radiation on the sample is masked by the large concentration of free current carriers already available. The copper sample which exhibits photoconductivity, for instance, has a resistivity at $-125^{\circ}$C of about $2 \times 10^{8}$ ohm-cm, whereas another copper sample (with no observable photoconductivity) had a resistivity at $-125^{\circ}$C of only $8 \times 10^{5}$ ohm-cm. Other typical resistivities of samples which did not show photoconductivity are:

Ag doped: p-type ($-100^{\circ}$C) $10^{7}$ ohm-cm

In doped: n-type ($-125^{\circ}$C) $10^{4}$ ohm-cm

e. Pure CdTe Samples: Indium electrodes were vacuum plated onto the samples cut from a pure CdTe crystal. Their variation in resistivity as a function of temperature was measured and plotted as $\ln \rho$ vs $1/T$ (figure 19a and b). Since from statistics, the resistivity of a semiconductor will vary as $e^{E/2kT}$, the relationship $\rho = Ae^{E/2kT}$ can be used to find the activation energy for the process of raising an electron out of the valence band into the conduction band and leaving a free hole behind. From this relationship we can get $\ln \rho = \ln A + (E_g/2kT)$ where $E_g/2k$ will be the slope of the line from which $E_g$ can be obtained. Values of 1.48 eV were obtained as the intrinsic energy gap for both of these samples. Since the lower temperature, or extrinsic values, of these two samples vary so greatly and do not give good straight lines they are probably indicative of leakage resistances encountered in measuring extremely small currents at very low temperatures.

In an effort to determine the most suitable electrodes for photoconductivity measurements the photo-response of these two samples was measured at room temperature (figure 20a and b). The indium electrodes were then removed from sample no. 2 and replaced with gold contacts. The thermal activation energy and photo-response were then measured and as can be seen from figure 19b the activation energy was lowered considerably below the generally accepted value obtained with other electrode materials, and the photoconductivity was completely destroyed, even at liquid nitrogen temperature. Removal of the Au contacts and about 0.5 mm of the crystal ends followed by replating with In only very slightly restored the photoconductivity. This sample was not used further for fundamental measurements as its exact composition was now in doubt, and In was adopted as the standard electrode for pure CdTe.

-56-

Resistance vs Temperature   Sample 1   (Dark)

Fig 19 A



Resistance vs Temperature   Sample 2   (Dark)
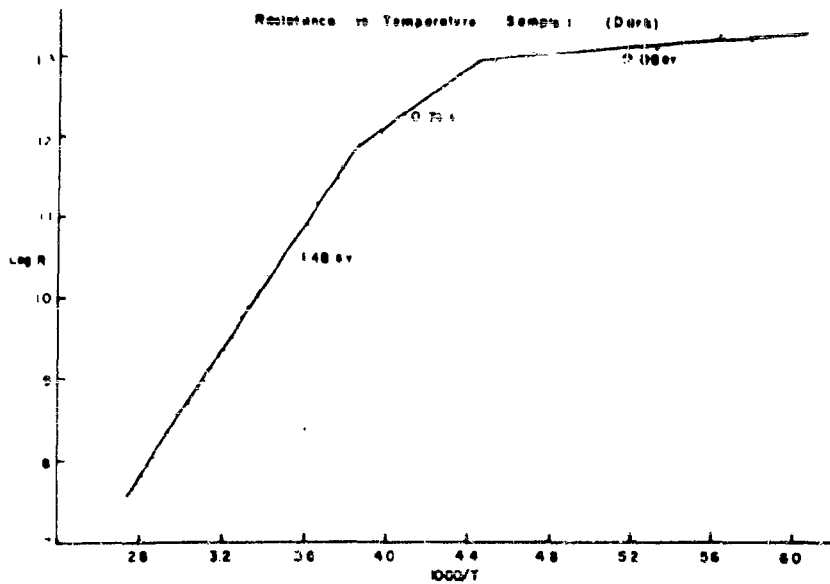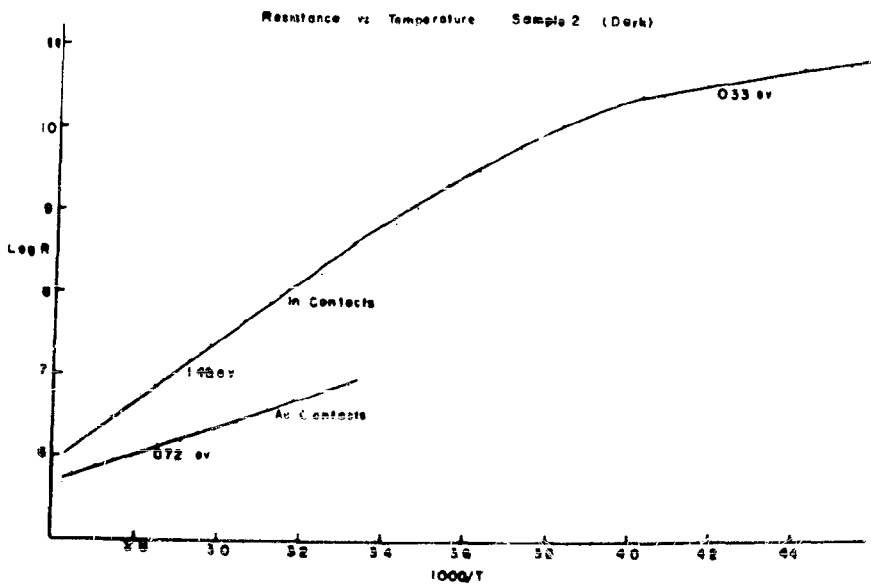
Fig 19 B

The intrinsic energy gap determined from figure 20 gives a value of 1.5 eV, in good agreement with thermal activation energy measurements. In figure 20a, and to some extent in 20b, a second apparent peak can be observed in the vicinity of 1.1 eV. There is also a difference in the photocurrent depending on the direction of radiation wavelength procession; i.e. short to long wavelength or long to short. With these considerations in mind, the photocurrent was measured using constantly changing wavelength radiation, in both directions, at a number of different temperatures. In all cases the sample was cooled in the dark, before being illuminated. It can be seen in figures 21 and 22 that the second peak is clearly resolved at 273°K and the shape and relative heights of the curves are greatly dependent on temperature. Figure 22 gives all the curves drawn on the same current axis to better show their relation to each other and represent photocurrent when the radiation wavelength was changing from short to long.

It was further observed at low temperatures, starting at 273°K, that rise and decay times started increasing. Because of this, further current measurements were made under constant wavelength radiation in order to assure equilibrium. It was first necessary to determine the shift in activation energy of each peak with temperature as shown in figure 23 to know what wavelength radiation to use. The figures for the intrinsic peak agree very well with absorption measurements of Bube (54) and dielectric measurements of Bailey (58). Measurements of the second peak were less conclusive, indicating the shift may be partly real and partly due to the relative change in shape and height of the two peaks.

Figure 24 shows a series of plots of maximum photocurrent vs relative intensity for each peak, using constant wavelength illumination, at different temperatures. In all cases the procedure for taking the data consisted of (1) cooling the crystal in the dark to the desired temperature,

-57-

1/R vs Wavelength Sample 2 (25°C)
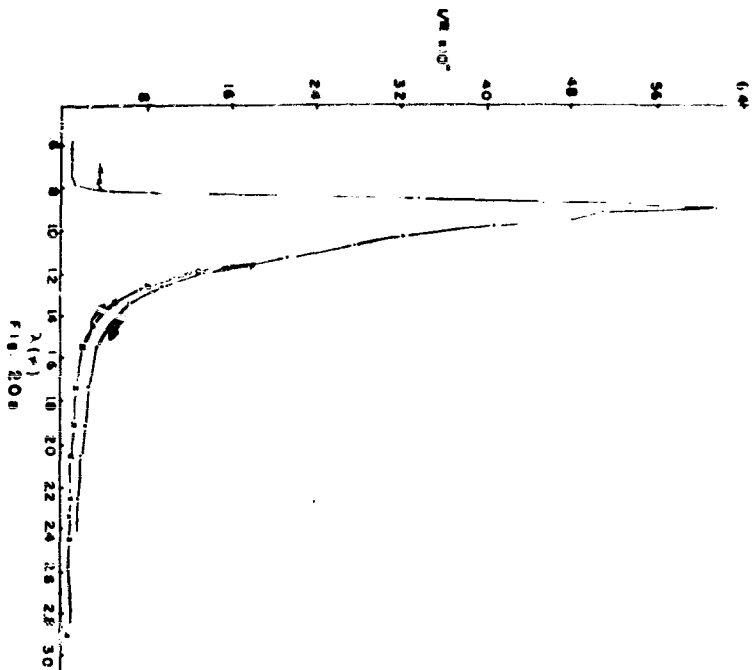
λ(μ)

Fig. 20B

1/R vs Wavelength Sample 3 (25°C)

λ(μ)

Fig. 20A

PHOTO CURRENT vs. WAVELENGTH
SAMPLE NO. 4
−125 °C

Fig. 18

PHOTO CURRENT vs. WAVELENGTH
SAMPLE NO. 1   350 °K

Fig. 21a

320 °K

Fig. 21b

300 °K

Fig. 21c

273 °K

Fig. 21b



240 °K

Fig. 21a



220 °K

Fig. 21f



180 °K

Fig. 21e

Fig 22

SHIFT OF II av. PEAK WITH TEMP.

λ (μ)

Temp (K)
Fig. 23b

SHIFT OF I50· PEAK WITH TEMP.

λ(μ)

$\lambda = 8100 + 2.08 T \, \text{Å}$

$\Delta e = 1.53 - .00035 T \quad e_V$

Temp. (°K)
Fig. 23 a
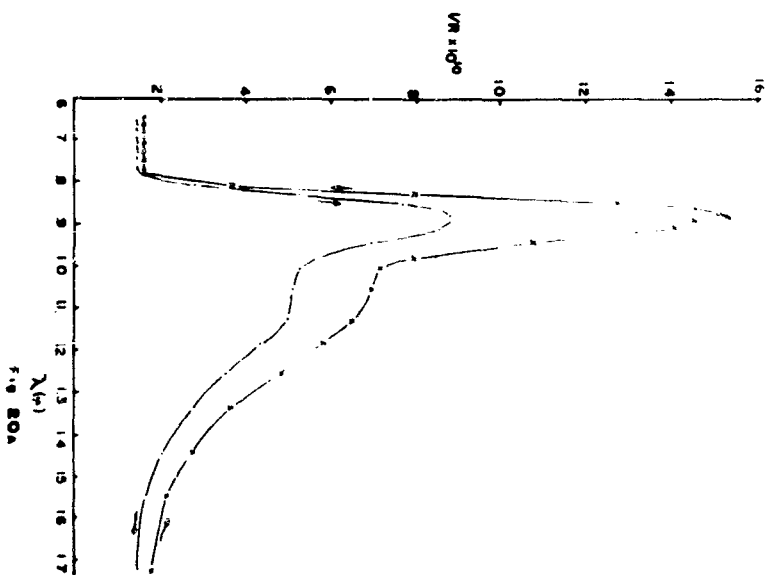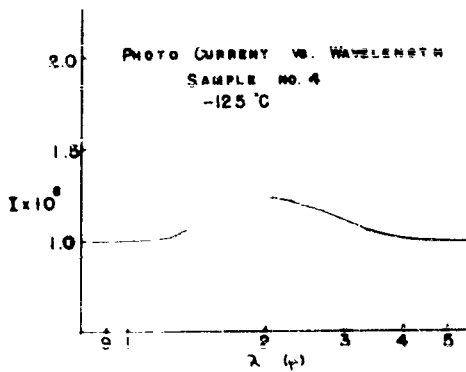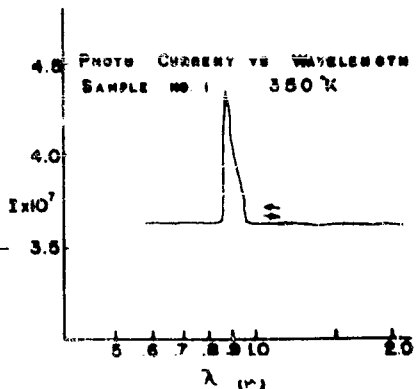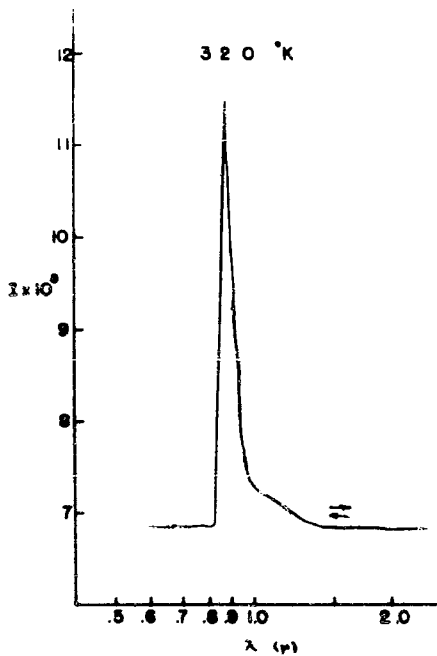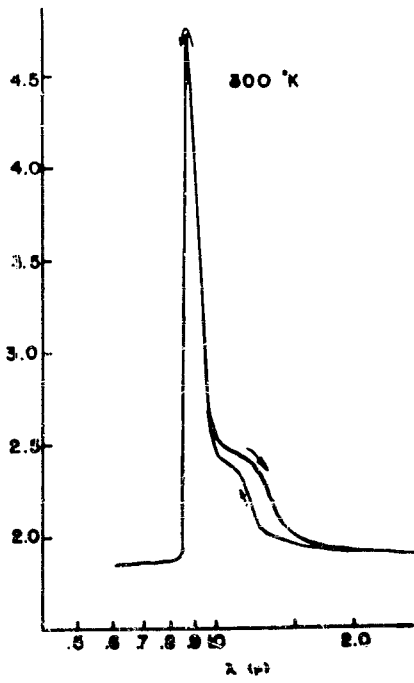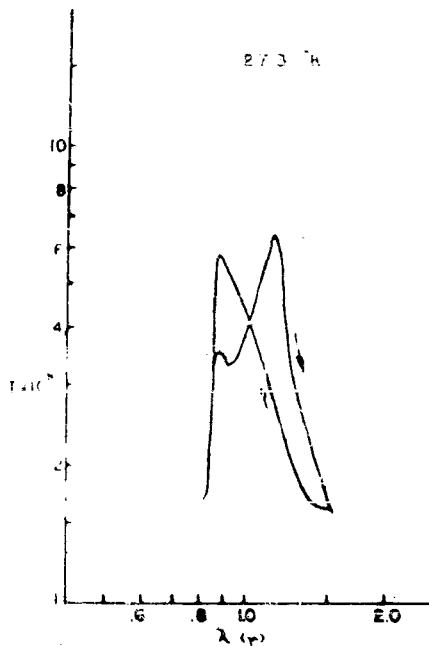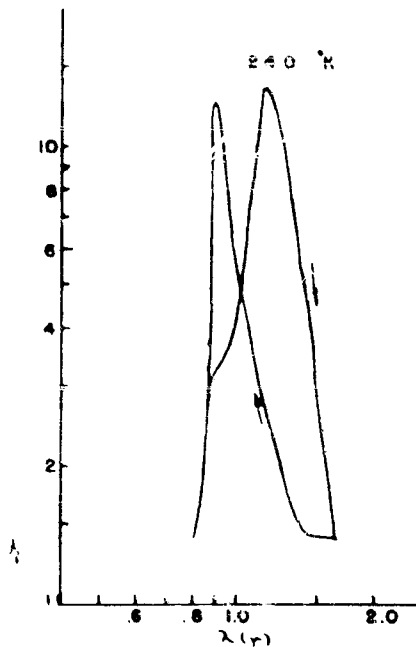
Photocurrent vs Light Intensity
1.5ev Peak
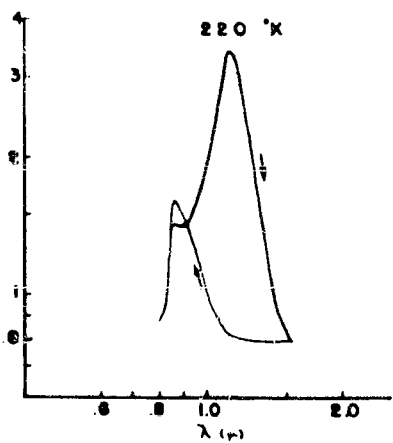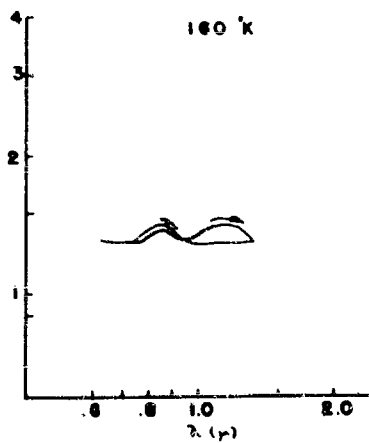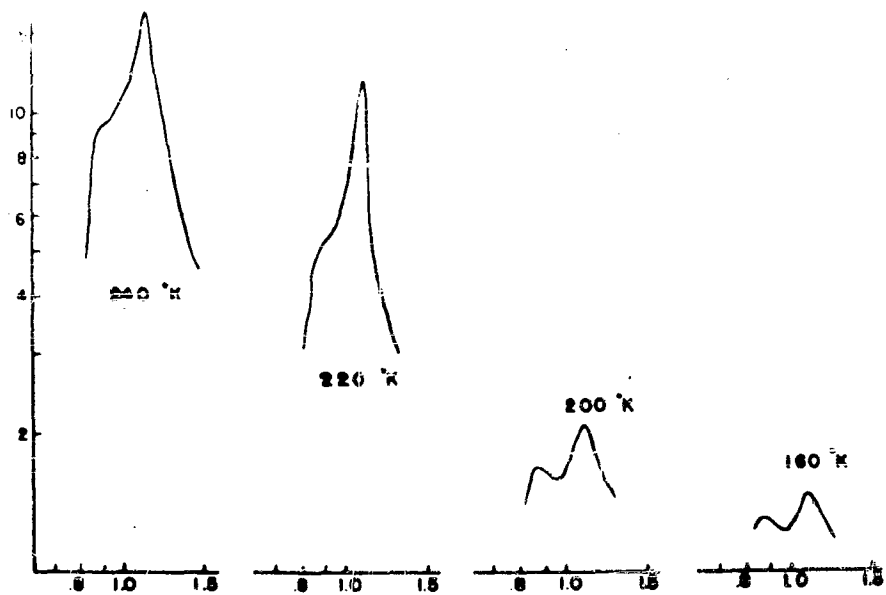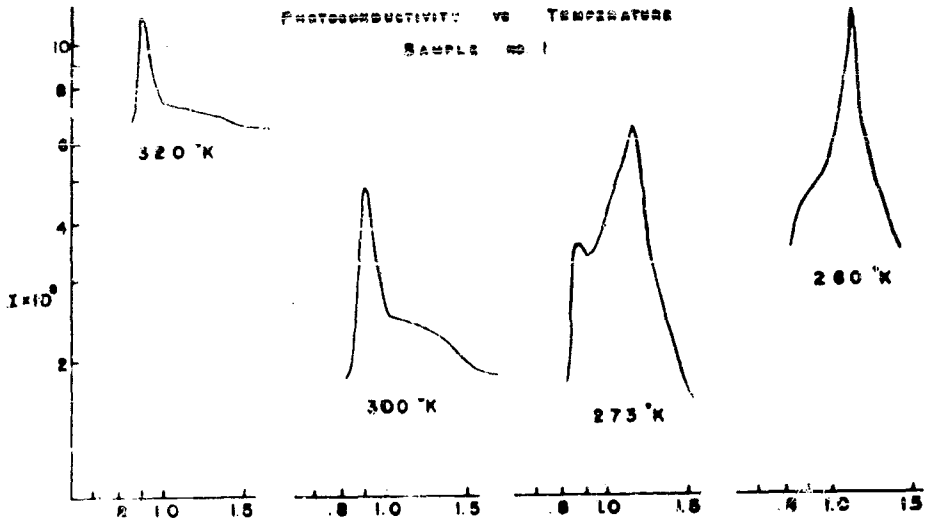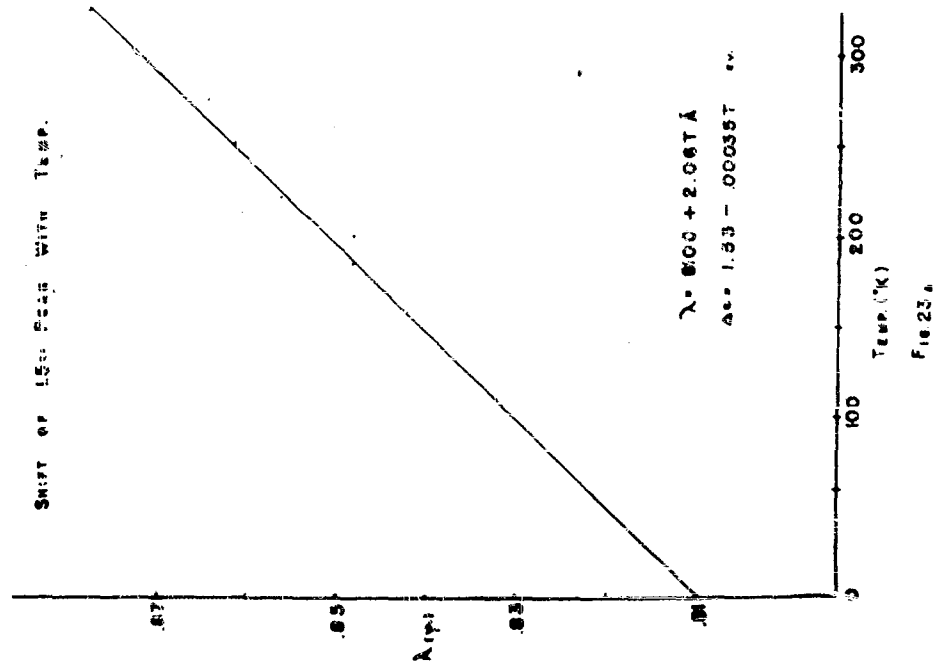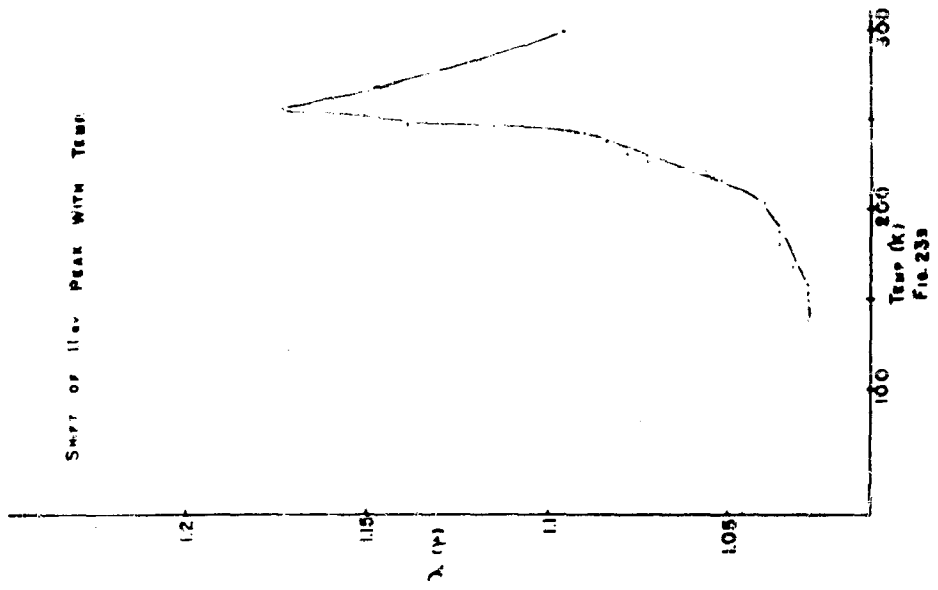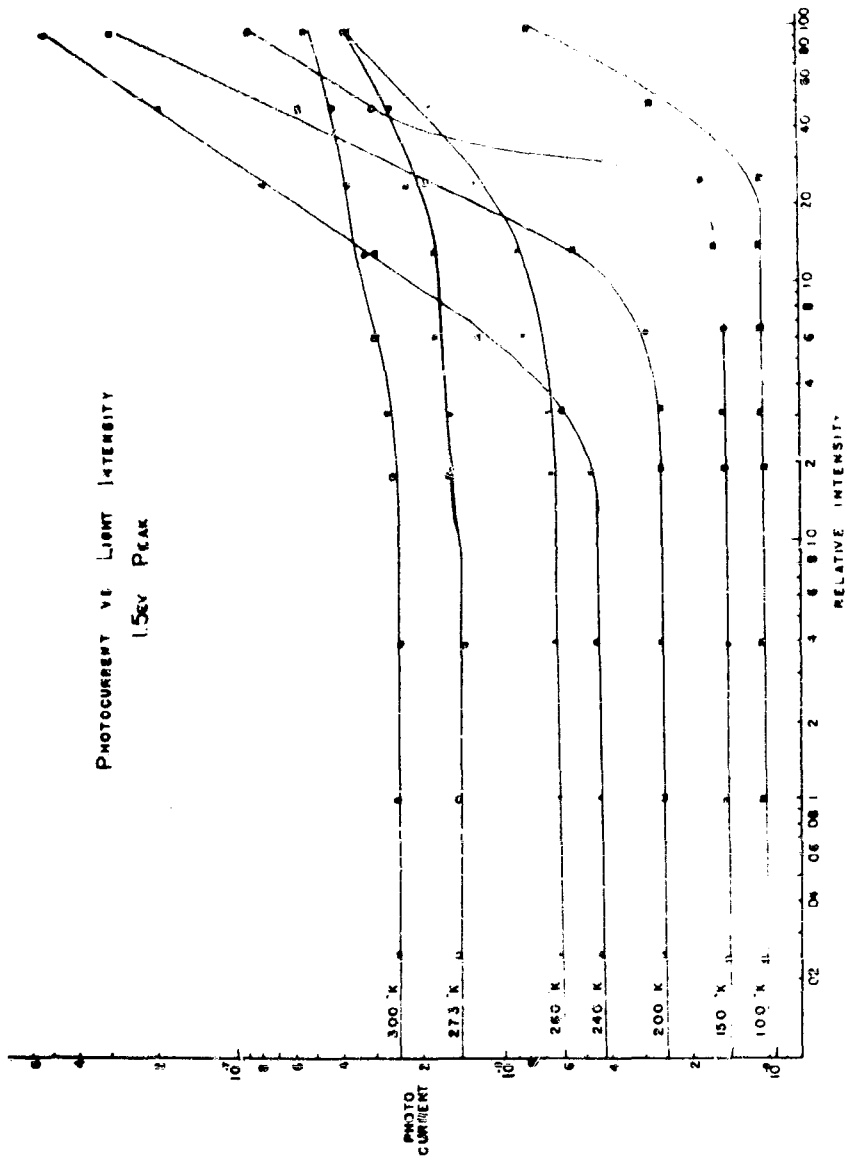
Fig 24.

PHOTOCURRENT vs LIGHT INTENSITY

11 EV PEAK

Fig 24₈

RELATIVE INTENSITY

PHOTO CURRENT

300 °K

273 °K

240 °K

240 °K

200 °K

150 °K

100 °K
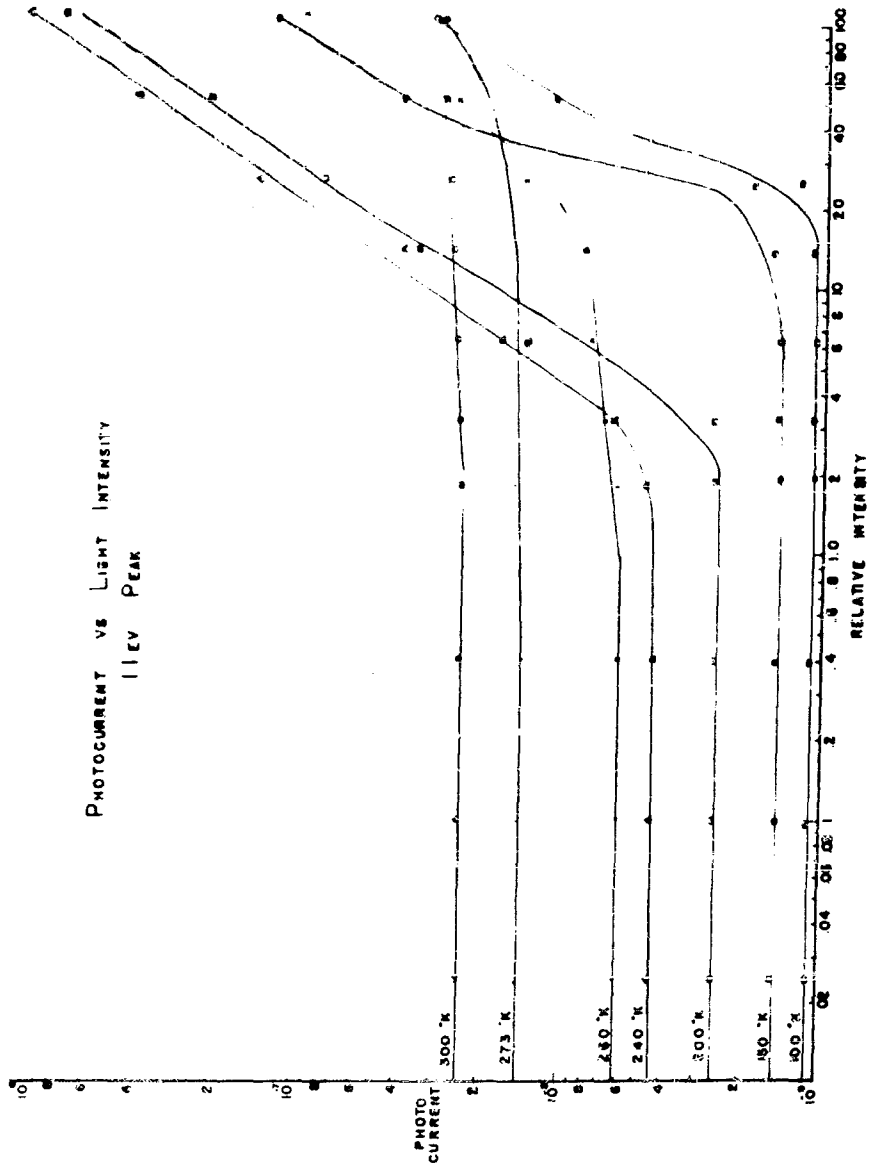
(2) obtaining an equilibrium dark current, (3) measuring equilibrium current due to 1.5 eV radiation behind 2.4 density filter, (4) changing to 1.1 eV radiation and measuring equilibrium current, (5) letting current return to dark value before repeating steps 3 and 4, with lesser densities.

The intensities were selected by the proper combination of 0.0, 0.3, 0.6, 0.9, and 1.2 neutral density filters. During this series of measurements it was observed that at 260°K the photocurrent due to 1.5 eV radiation exhibited a rise time of some few minutes. Upon interruption of illumination, however, the decay was rather rapid. As the temperature was lowered further the rise time increased to about 12 minutes at 240°K, 20 minutes at 200°K, and 40 minutes at 180°K. Rise time for the 1.1 eV peak was rather short in all cases. It was further observed that if illumination were continued after the intrinsic maximum was reached, the current would commence very slowly to decrease. If this were allowed to continue for a few minutes before the radiation was changed to 1.1 eV, the 1.1 eV peak would be considerably lower than if the radiation wavelength were changed immediately when the maximum was reached. With such long rise times it was difficult to establish exactly when the maximum had been reached and so certain of the 1.1 eV readings are somewhat low. This may account in part for the scattering of data in the low temperature, low intensity readings. The measurements at 0.0 and 0.3 density (100 and 50 relative intensity) are probably more reliable and some significance may be attached to their form.

Decay times also increased at lower temperatures, to such an extent that at 200°K it was necessary to return the sample to room temperature and re-cool between each different intensity reading.

It had earlier been noted that samples left for long periods in the dark at room temperature seemed to become activated by illumination. That is, if they were swept by radiation changing back and forth from energies greater than 1.4 eV to less than 1.1 eV, although dark current would return to its original value between each pass, their photocurrent would become larger each time. It was felt from the previous measurements that this effect should become larger at low temperatures and in fact it did. A sample was cooled to 240°K in the dark where it had a dark current of $4.3 \times 10^{-7}$ amps (100 volts). It was then illuminated with 1.5 eV radiation which caused its current to rise to $460 \times 10^{-9}$ amps in ten minutes at which time it became steady. The radiation was changed to 0.7 eV and then back and forth between 0.5 and 1.6 eV. The following tabulation gives photo-current as the radiant energy passed through each peak. No values are given for the 1.1 eV peaks for wavelength changing from long to short as the photocurrent in this instance is merely rising to its intrinsic peak as shown in figure 21.

| Wavelength | 1.5 eV | 1.1 eV |
|---|---|---|
| s ——→ l | $460 \times 10^{-9}$ | 440 |
| ←—— | 710 | --- |
| ——→ | 640 | 1040 |
| ←—— | 670 | -- |
| ——→ | 850 | 1140 |
| ←—— | 920 | --- |
| ——→ | 880 | 1180 |
| ←—— | 960 | --- |
| ——→ | 890 | 1270 |

Table 2

Thermal glo-curves, as reported by various workers (?,?,et al) for a wide variety of photoconductors and phosphors, were obtained for pure CdTe single crystals. Figure 23 shows a plot of the thermally stimulated current against temperature. The following procedure is used to obtain these curves.

1. The crystal is warmed until it is well into its intrinsic conductivity region, i.e., all the levels in the forbidden gap are essentially empty. For this particular sample about 40°C was taken as the appropriate temperature.

2. Cool in the dark to liquid air temperature (77°K).

3. Illuminate with radiation of energy equal to the intrinsic activation energy at that temperature, until an equilibrium current is obtained. For CdTe this was 8260 Å corresponding to an energy of 1.50 eV.

4. Remove radiation and allow any rapid decay in photocurrent to take place.

5. Warm at steady rate in the dark. This rate is quite arbitrary and rates of from ? to 14 degrees per minute have been reported. The rate used here was about 10 degrees per minute. The difference between the current on warming and cooling is the thermally stimulated current.

The magnitude of this current was found to be strongly dependent on time of illumination. Below 190°K the actual photocurrent, as mentioned earlier, is quite small and its rise time quite long. Because of this it is difficult to know exactly when equilibrium conditions are obtained in step 5. As can be seen from figure 24, there is a large burst of thermally stimulated current in the region of -30 to + 10°C.

THERMAL GLO-CURVE

SAMPLE NO. I

TEMP. (°C)
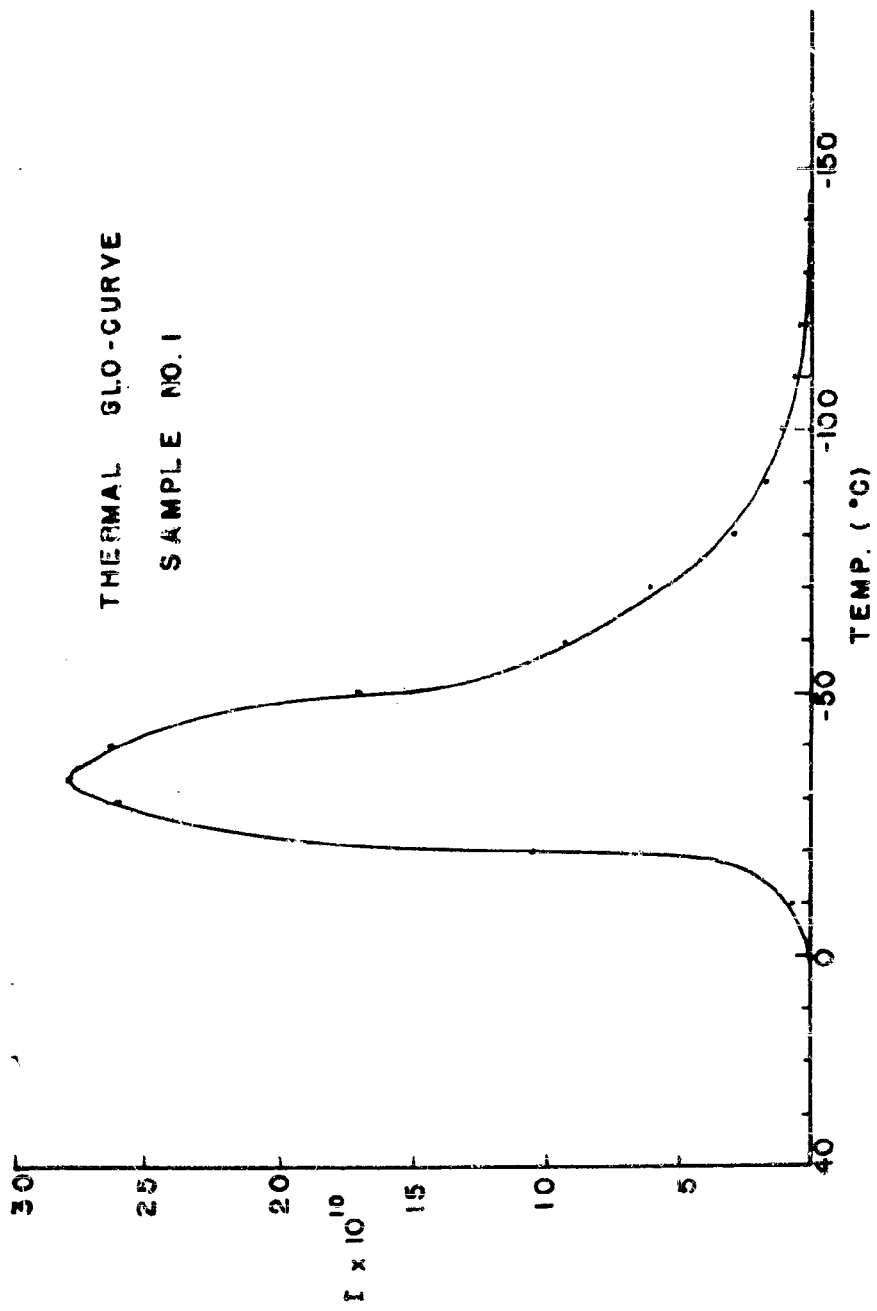
FIG. 25

4.3 Discussion of Results

(a) Copper Doped Crystals: The information obtained from photo-conductivity measurements of copper doped CdTe single crystals gives little insight into the properties of CdTe itself. It does indiate, however, that Cu ions, substituted for Cd, gives rise to a set of levels about 0.65 eV above the valence band. At room temperature the concentration of unfilled ground states which will act as recombination centers is sufficient that the **net** number of free carriers liberated by 1.6 eV illumination will be so small as to not measurably affect the already high conductivity. If we assume that all of 0.1 mole percent copper added to the crystal batch is reasonably uniformly distributed throughout the crystal this means a concentration of copper ions on the order of $10^{20}$ cc$^{-1}$. Even allowing for segregation during crystal growth, the density of these states will probably approach $10^{19}$ cc$^{-1}$. The number of free holes created by electrons being raised up to the 0.65 eV level by 1.65 eV radiation will likewise be small compared to the number of free carriers already present and so no impurity photoconductivity occurs.

As the temperature is lowered, however, the concentration of empty states at 0.65 eV above the valence band increases, decreasing the number of holes in the valence band. This decrease, however, is still not sufficient to affect the concentration of current carriers under intrinsic illumination, and so no photocurrent is yet observed. This might also be regarded as an increase in the concentration of empty re-combination centers with the resultant decrease in carrier lifetime, which would also prevent photoconductivity from being observed. If the first case were true one might anticipate finding intrinsic photoconductivity at lower temperatures, although none is found as low as $-180^{\circ}$C, whereas the second case precludes this possibility. The fact that photoconductivity

-61-

does occur under 0.65 eV radiation below about -125°C, which indicates the concentration of free current carriers (holes) does in fact increase, lends support to the latter case. This, of course, anticipates near equal rates of excitation for the two wavelengths.

While it might be anticipated that photoconductivity due to 0.85 eV radiation (1.45$\gamma$ ) might also be encountered, arguments similar to those above can account for its absence. At room temperature the net concentration of carriers raised to the conduction band will be small compared to those already there and at low temperatures the concentration of empty recombination centers will prevent a noticeable increase in carrier concentration. It was suspected that the increase in the concentration of filled ground states at low temperature resulting from 0.65 eV radiation might result in a photocurrent due to 0.85 eV illumination if this closely followed the 0.65 eV radiation. This effect, as can be seen from figure 18, was not observed.

b. Pure CdTe Single Crystals: The band model for CdTe as determined from the previously described measurements is proposed to be that shown in figure 26.
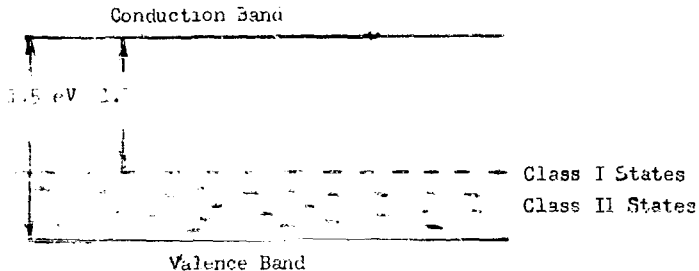


Figure 26

From the known purity of the starting materials and the fact that intrinsic semiconductivity in CdTe had not previously been reported below about 400°K, whereas these crystals were intrinsic down to about 250°K, we can assign an impurity concentration of about $10^{17}$ cc$^{-1}$ to these samples. These levels at 0.4 eV above the valence band and the states scattered between them will be essentially full at room temperature.

Photoeffects due to radiation of different energies and applied in different orders at a variety of temperatures can now be discussed in a semi-quantitative manner by use of this model.

350°K Temperature Range: At this temperature, intrinsic conductivity gives a dark current of about $3.6 \times 10^{-7}$ amps, which rises to $4.25 \times 10^{-7}$ amps under 1.5 eV illumination. The change in conductivity due to 1.1 eV will be immeasurably small because of the large concentration of thermally excited carriers compared to the number excited by radiation. Illumination of 1.5 eV energy, however, is acting on a greater concentration of electrons available for excitation and so a small photocurrent is produced.

300°K Temperature Range: Here the dark current has decreased to $1.8 \times 10^{-8}$ amps and a significant photocurrent is beginning to appear from the 0.4 eV level. With the appearance of photoconductivity due to 1.1 eV illumination the beginning of effects due to direction of wavelength (energy) change is observed. As the conduction band becomes thermally emptied the effect of intrinsic radiation also increases.

273°K Temperature Range: The crystal is now entering the transition range in the thermal activation energy plot (figure 19) and the dark current has decreased only slightly to $1.5 \times 10^{-8}$. The accompanying decrease in intrinsic conductivity results in a much greater contribution to the photoconductivity from the 0.4 eV level, and the effect of wavelength

-61-

procession has become quite pronounced. This is readily explained as follows: in going from long to short wavelength the crystal first experiences illumination from 1.1 eV radiation. Since the 0.4 eV level is being thermally emptied the slight increase in photocurrent due to this level "blends in" with the rise of the intrinsic photocurrent. As the radiation changes to higher energies the current increases until a maximum is reached at 1.5 eV. If, on the other hand, the illumination is started from the high energy end, electrons are first excited by 1.5 eV radiation from the valence band into the conduction band and the photocurrent quickly reaches a maximum. This maximum is much lower than the previous maximum because many electrons are quickly trapped in the now partially empty 0.4 eV levels and shallow traps. That is, the exciting radiation is proceeding from a region of high density of "excitable" electrons to a region of lower density.

Since the concentration of filled 0.4 eV levels has now been increased, when the radiation changes to 1.1 eV, the current may be greater than with 1.5 eV illumination.

This effect is very clearly demonstrated by varying the radiation between 0.95 and 1.18 (1.36 to 1.03 eV), in which case the photocurrent due to 1.1 eV radiation is the same in both directions. The photocurrent from 1.5 eV illumination is also the same in both directions when the radiant energy is varied between 1.6 and 1.2 eV.

220°K Temperature Range: The 1.1 eV peak is now completely absent when going from low to high energies; i.e. the 0.4 eV level has been thermally emptied. The decrease and final disappearance of this peak is accompanied by a steady decrease in the intrinsic peak and increase in the 1.1 eV peak when the radiation starts at the high energy end. This further indicates that electrons excited by 1.5 eV radiation

are in fact trapped out in the 0.4 level. Since the concentration of
filled 0.4 eV levels is now so much greater than the net concentration of
free carriers placed in the conduction band by intrinsic radiation the
photocurrent will be much larger due to 1.1 eV illumination.

The rise of intrinsic photoconductivity starting with energies
slightly higher than 1.1 eV shows, however, that some of the levels below
the 0.4 level are still normally filled at this temperature.

As the crystal is cooled further these levels are also thermally
emptied until at 160°K there is only a small amount of photoconductivity
in the immediate region of each peak.

It was later observed in taking the data of figure 21 using
constant wavelength illumination that the photocurrent at low temperatures
exhibits extremely long rise times (up to one hour) and even longer decay
times (several hours) so the actual peak heights may be somewhat greater
than shown in figures 21 and 22, and the dark current may be lower. The
following tabulation, however, shows that the trends indicated by figures
21 and 22 are followed even with constant wavelength allowing equilibrium
current to attain.

<div align="center">Table 3</div>

| Temp.°K | Dark Current | Changing | | Constant | |
|---|---|---|---|---|---|
| | | 1.5 eV | 1.1 eV | 1.5 eV | 1.1 eV |
| 350 | $4.6 \times 10^{-7}$ | $4.25^*$ | $3.6^*$ | $4.25^*$ | $3.6^*$ |
| 320 | $6.6 \times 10^{-8}$ | 11 | 7.1 | 11 | 7.1 |
| 300 | $3.4 \times 10^{-8}$ | 4.7 | 2.4 | 5.0 | 2.4 |
| 273 | $1.4 \times 10^{-8}$ | 3.5 | 6.0 | 4.05 | 3.0 |
| 240 | $4.4 \times 10^{-9}$ | 30 | 165 | 560 | 1000 |
| 200 | $2.6 \times 10^{-9}$ | 15 | 22 | 308 | 750 |
| 120 | $1.5 \times 10^{-9}$ | 12 | 15 | 35 | 120 |
| 100 | $1.1 \times 10^{-9}$ | | | 7.7 | 25 |

*figures in these columns are x same factor of 10 as dark current

The data presented in figure 2a and b show CdTe exhibits a
slightly supralinear photo-response, with varying light intensity,
starting at about 77K. This can be interpreted on the basis of earlier
discussion by means of assigning equal capture cross sections for elec-
trons and holes to the 0.6 eV levels and larger capture cross section for
holes than electrons to those levels scattered below 0.6 eV. Under 1.4 eV
radiation the 0.6 eV levels become saturated with electrons at high light
intensities since the other levels have a small probability for electron
capture and are increasing in concentration with increasing radiation
intensity. This results in a photocurrent vs light intensity plot with a
power greater than unity.

The photocurrent induced by 1.1 eV radiation also increases in
a supralinear manner and can be explained on a similar basis. Since these
currents were measured immediately following the photocurrent due to 1.4 eV
radiation the 0.6 eV levels and particularly those below them were essen-
tially full, leaving a large concentration of holes in the valence band.
Under 1.1 eV radiation electrons are raised to the conduction band from
the 0.6 levels. The class II states between the 0.6, or class I states,
and the valence band at the same time are capturing holes which are recom-
bining with electrons in these states. The class I states will be in
optical equilibrium with the conduction band and since some electrons will
also be excited from the class II states due to their proximity to the class
I states, these class I states will again become saturated with electrons
and lead to a supralinear photocurrent.

The long rise and decay times encountered at the temperatures
where **supralinearity** occurs can then be accounted for as the time necessary
to cause the redistribution of electrons and holes in the two different
states.

The effect observed in connection with State I can be attributed
to this same [illegible]. One cycle from 1.8 eV to 1.5 eV and back to
1.8 eV can be explained. The [illegible] 1.5 eV radiation causes a photocurrent
which rises to a steady value and at the same time refilling first the [illegible]
I and II states which capture the electrons raised to the conduction band.
When the radiation is changed to 1.1 eV a large photocurrent is obtained,
as previously shown, and simultaneously a redistribution in electron and hole
concentration in the class I and II states occurs as in the case of super-
linearity. This results in an even larger photocurrent from intrinsic radia-
tion since a large concentration of possible traps is already full. If the
cycle is repeated rapidly the original distribution cannot be thermally
restored and we have a "sensitization" of the crystal by radiation similar
to that described earlier. It might be anticipated that the maximum values
obtained from this series of reversals would be equal to the maximum obtained
by steady illumination. If we compare data in tables 2 and 3 we see that
the value for steady 1.1 eV radiation is [illegible] compared with 950 x 10^{-7}
and 1000 x 10^{-7} compared to 1100 x 10^{-7} for 1.1 eV. Taking into account
the long rise times encountered in the steady illumination data the agree-
ment is fairly good.

The thermal glow-curves also indicates the presence of a set of
deep traps in the forbidden zone, which can be filled by electrons "liberated"
by radiation. While the exact energy of these levels cannot be determined
directly from these curves the fact that they are not thermally emptied
until about 250°K indicates they are a considerable distance (energy wise)
below the conduction band. These levels then should be those located at
0.4 eV above the valence band as determined in the previous discussion.

A "blank" run was also made on this sample, that is, it was cooled and warmed in the dark with no illumination in between. No thermally stimulated current was observed in this case, which further supports the contention that the ... eV states are essentially empty in the dark at ... temperatures.

Throughout all the measurements it was impossible to observe a photocurrent due to ... (V) radiation even under circumstances which called for this level to be empty and transition be avoid electrons. A positive interpretation of this may be made on the basis of directional properties of band structure. It is very possible that the shortest distance from the valence to the conduction band or the levels in the forbidden gap is not a line of constant k. That means that in order to undergo such a transition, a change in the wave number vector k, which is defined in terms of the reciprocal lattice, must occur along with an increase in energy. This necessitates a change in direction and hence momentum. If the momentum of a photon and free electron are compared it can be seen that the conservation of momentum will prevent the photon from appreciably changing the momentum of the electron which it strikes.

### Momentum of a 1 eV photon

$$E = h\nu = pc$$

$$p = \frac{h\nu}{c} = \frac{h}{\lambda}$$

$$p = 6.6 \times 10^{-27} \text{ erg sec} \times \frac{1}{6.3 \times 10^{-5} \text{ cm}} = 1.07 \times 10^{-22} \frac{\text{erg sec}}{\text{cm}}$$

since 1 erg = 1 dyne cm = $1 \frac{\text{gm cm}^2}{\text{sec}^2}$

$$mv = 1.1 \times 10^{-22} \frac{\text{gm cm}}{\text{sec}}$$

### Momentum of a Free Electron

$$mv = 0.9 \times 10^{-27} \text{ gm} \times 10^8 \frac{\text{cm}}{\text{sec}} = 10^{-19} \frac{\text{gm cm}}{\text{sec}}$$

Thus we see than an electron will have about $10^3$ times the momentum of a 2 eV photon. Phonon interaction in the lattice, on the other hand, possess sufficient momentum to be able to change the momentum of electrons.

If the defects giving rise to these levels 1.4 eV above the valence band are located such that electrons require a change of momentum to be raised up to them, then we would not expect to observe a photocurrent from 0.4 - 1.4 eV excitation. We would, however, expect this thermally filled at higher temperatures as is the case.

## 5.1 Zone Refining

The technique of zone refining has been found to be eminently satisfactory for the production of ultra-pure tellurium, selenium, and sulfur. Fifty passes at a rate of travel of two inches per hour, using one inch wide heaters on four inch centers, produced material of sufficient purity for the growth of semiconductor single crystals with an impurity content of about $10^{-7}$ cc. The difference in final purity level after about 50 passes was almost the same regardless of whether the starting material was high purity or ordinary C. P. grade.

Containers of fused alumina proved to be superior to fused silica or "Vycor" for this process from a durability point of view and were not at all objectionable from a purity standpoint. An atmosphere of high purity helium maintained over the melt prevented contamination of the molten zones from the surroundings.

## 5.2 Crystal Growth

High purity single crystals of CdTe and ZnTe suitable for photoconductivity measurements were produced by a modified Stockbarger furnace. Very robust containers, consisting of heavy walled fused silica tubes encased in a fused alumina tube, were needed to contain the pressure of the melt during crystal growth. Even this did not prove reliable for ZnTe although it was quite dependable for CdTe. A tight fitting casing of graphite with a screw top was attempted to hold the ZnTe and with modifications might prove useful.

Temperature was controlled by platinum resistance thermometer temperature controllers to within $\pm 0.5°C$ at $1000°C$ over the three or four days necessary for crystal growth. Using a growing rate of two mm

per hour and an annealing rate of 25 degrees per hour, a success ratio of about 60% was obtained in growing CdTe, both pure and doped. Crystals were grown containing one mole percent indium, silver, and copper. The indium-doped crystals showed n-type character, while silver-doped, copper-doped and pure crystals were p-type as indicated by thermal emf measurements.

## 9.2 Photoconductivity

Some photoconductivity properties of CdTe single crystals have been measured and a band model proposed to explain the results. Pure CdTe exhibits photoconductivity at two different wavelengths, 0.80μ and 1.1μ; the first being intrinsic photoconductivity, and the second arising from the location of levels 0.4 eV above the valence band. Both peaks shift with temperature although the actual shift of the second peak is confused by a change in relative heights of the two peaks, and their overlap. The intrinsic activation energy shifts according to the following:

$$\Delta = 1.5 - 0.00035T \quad \text{eV}$$

The states 0.4 eV above the valence band are proposed to be analogous to those located 0.6 eV and 1.0 eV above the valence band in pure CdSe and CdS respectively. The band model proposed is based on the semi-quantitative theoretical considerations of recombination given by Rose which have been shown to have a more precise mathematical interpretation for CdS and CdSe, and involves two types of recombination centers. The levels at 0.4 eV are assigned equal capture cross section for electrons and holes and the quasi-continuum of discrete levels scattered between this level and the valence band are given a larger capture cross section for holes than for electrons. This arrangement of recombination centers can account for the supralinearity of both the 1.5 and 1.1 eV photocurrents and for their rise times. The shift in magnitude of the two photocurrents

with temperature and direction of wavelength change can also be explained on this basis. No photocurrent was ever observed corresponding to 0.4 eV and is explained on the basis of the directional properties of band structure.

REFERENCES

1.  B. Gudden and R. W. Pohl, Z. Physik 2, 181, 46. (1920); 1, 48 (1920).

2.  W. C. Ellis, Trans. Am. Inst. Mining Met. Engrs., 18, 22 (1952).

3.  C. W. Horton, R. C. Frin, W. E. Blmeter, J. Chem. Phys., 41, 1937 (1949).

4.  C. D. Thurmond and J. D. Struthers, J. Phys. Chem., 57, 81 (1953).

5.  A. Hayes and J. Chipman, Trans. Am. Inst. Mining Met. Engrs., 135, 85 (1939).

6.  see number 1

7.  D. F. Detwiler and W. M. Fox, Trans. Am. Inst. Mining Met. Engrs. 203, 205 (1955).

8.  P. H. Keck and G. J. E. Golay, Phys. Rev. 89, 1927 (1953).

9.  W. G. Pfann and J. H. Hagelbarger, J. Appl. Phys. 27, 12 (1956).

10. P. H. Brace, A. W. Reinert, and G. Schwartz, Rev. Sci. Inst. 26, 303 (1955).

11. P. Curie, Bull. Soc. Franc. Mineral., 8, 145 (1885).

12. H. E. Buckley, "Crystal Growth", John Wiley & Son, New York, 1951.

13. H. Hilton, "Mathematical Crystallography", Clarendon Press, Oxford, 1903.

14. G. Wulff, Z. Krist. 34, 449 (1901).

15. A. Berthoud, J. chim. phys. 10, 624 (1912).

16. F. C. Frank, Disc. of Faraday Soc. 5, 48 (1949).

17. W. G. Pfann, "Solid State Physics, Vol. 4", Academic Press, New York, 1957.

18. G. Tammann, "States of Aggregation", Van Nostrand, New York, 1925.

19. J. W. Rutter and B. Chalmers, Can. J. Phys. 31, 15 (1953).

20. C. Wagner, Trans. Am. Inst. Mining, Met. Engrs. 200, 154 (1954).

21. C. S. Barrett, "Structure of Metals", 2nd. ed., McGraw-Hill, New York, 1952.

22. G. Tammann, "Metallography", The Chemical Catalog Co., New York, 1925.

23. P. W. Bridgman, Proc. Am. Acad. Arts, Sciences, 60, 303 (1925).

24. D. C. Stockbarger, Rev. Sci. Inst. 7, 133 (1936).

25. P. Kapitza, Proc. Roy. Soc. (London) A119, 358 (1928).

26. J. Czochralski, Z. physik. Chem. 92, 219 (1918).

27. Roth and Taylor, Proc. I.R.E., 40, 1348 (1952).

28. S. Kyropoulas, Z. anorg. u. allgem. Chem. 154, 308 (1926).

29. G. K. Teal and J. B. Little, Phys. Rev. 78, 647 (1950).

30. W. W. Bradley, "Transistor Technology", Vol. 1, Van Nostrand, Princeton, N.J., in press.

31. A. Verneuil, Ann. Chim. Phys. series 8, 3, 20 (1904).

32. D. M. Heinz and E. Banks, J. Chem. Phys. 24, 391 (1956).

33. Bishop and Liebson, J. Appl. Phys. 24, 660 (1953).

34. R. Frerichs, Phys. Rev. 72, 594 (1947).

35. D. Jenny and R. Bube, Phys. Rev. 96, 1190 (1954).

36. E. A. Kroger and H. de Nobel, J. Electronics 1, 190 (1955).

37. B. Gudden and R. Pohl, Z. Physik. 16, 384 (1923).

38. A. Rose, Phys. Rev. 97, 322 (1955).

39. R. Bube, J. Phys. Chem. Solids. 1, 234 (1957).

40. H. Holteckscher, J. Opt. Soc. Am. 47, 765 (1957).

41. A. Rose, RCA Review, 12, 362 (1951).

42. R. Bube and S. Thomsen, J. Chem.Phys. 23, 15 (1955).

43. T. S. Moss, "Photoconductivity in the Elements", Academic Press, New York, 1952.

44. T. S. Moss, Proc. Phys. Soc. (London), B66, 993 (1953).

45. H. S. Sommers and R. E. Berry, Electroluminescence and Photoconduction Symposium, Brooklyn, 1955.

46. R. W. Smith, Phys. Rev. 93, 347 (1954); 98, 1169 (1954).

47. R. W. Smith, RCA Review, 12, 350 (1951).

48. R. Frerichs, Phys. Rev. 76, 869 (1949).

49. J. Lambe and C. Klick, Phys. Rev. 98, 909 (1955).

50. R. E. Halsted, Electroluminescence and Photoconduction Symposium, Brooklyn, 1955.

51. C. A. Duboc, Brit. J. Appl. Phys. 107, Suppl. No. 4 (1954).

52. J. Appel, Z. Naturforsch. 7a, 705 (1952).

53. Moglich and Rompe, Zeits. f. Physik, 119, 4.2 (1942).

54. R. Bube, Phys. Rev. 98, 431 (1955).

55. F. Van Doorn and D. de Nobel, Physica 22, 338 (1956).

56. R. W. Smith, Phys. Rev. 97, 1525 (1955).

57. E. A. Kroger, G. Diemer, H. Klasens, Phys. Rev. 103, 279 (.956).

58. P. C. Bailey, ONR Report, Nonr 1503(01) (1956).

59. S. Tutihasi, J. Opt. Soc. Am. 46, 443 (1956).

# Armed Services Technical Information Agency

## ARLINGTON HALL STATION
## ARLINGTON 12 VIRGINIA